Electronic Supplementary Material (ESI) for Polymer Chemistry.

Supporting Information

Tuning of Hydrogen Peroxide-Responsive Polymeric Micelles of Biodegradable Triblock Polycarbonates as a Potential Drug Delivery Platform with Ratiometric Fluorescence Signaling

*Ying-Hua Fu, Chun-Yen Chen and Chao-Tsen Chen**

Department of Chemistry, National Taiwan University, Taipei, Taiwan 106, ROC

* Address correspondence to chenct@ntu.edu.tw

TABLE OF CONTENTS

1. Materials and apparatus

2,2-Bis(hydroxymethyl)propionic acid (**bis-MPA**) and diethylene glycol monomethyl ether were obtained from Acros chemicals and used as received. [4-(4,4,5,5-Tetramethyl-1,3,2-dioxaborolan-2-yl)-phenyl]methanol and Nile red were purchased from Alfa Aesar and Sigma Aldrich, respectively. All other reagents and solvents were used as received unless otherwise noted. 5-Methyl-2-oxo-1,3-dioxane-5-carboxylic acid (**TMC-COOH**),[1] perfluorophenyl 5-methyl-2-oxo-1,3-dioxane-5-carboxylate (**TMC-OPhF5**),[2] 2-[4-(2-aminoethoxy)phenyl]-3-hydroxy-4H-chromen-4-one (**3-HFNH$_2$**),[3] 1-(3,5-bis(trifluoromethyl)phenyl)-3-cyclohexylthiourea (**TU**),[4] 3-[(*tert*-butyldimethylsilyl)oxy]propan-1-ol,[5] 1-(1-hydroxycyclohexyl)cyclohexan-1-ol[6] and 14-(iodomethyl)-13,15-dioxa-14-boradispiro[5.0.5^7.3^6]pentadecane[6] were synthesized according to the literature procedures, respectively. Dulbecco's modified eagle medium (DMEM), fetal bovine serum (FBS, qualified) and penicillin-streptomycin (PS, including 10000 unit/mL penicillin and 10000 μg/mL streptomycin) were purchased from HyClone (Thermo Scientific) and Gibco (Life Technologies), respectively. Trypan blue solution (0.4%) and ProLong® Gold anti-fade reagent were obtained from Sigma-Aldrich and Life Technologies, respectively. Premixed WST-1 cell proliferation reagent was purchased from Clontech Laboratories. RAW 264.7 murine macrophage cell lines were purchased from Bioresource Collection and Research Center (BCRC) (Hsinchu, Taiwan). Analytical thin layer chromatography (TLC) was performed with Merck Silica Gel 60 F_{254} glass plates pre-coated with a 0.25-mm thickness of silica gel and then monitored under UV light (254 nm) and visualized with phosphomolybdic acid (PMA) or potassium permanganate ($KMnO_4$) staining solutions. Flash chromatography was performed on Merck Silica Gel 60 (230-400 mesh) silica gel.

Proton nuclear magnetic resonance (^{1}H NMR) spectra and carbon nuclear magnetic resonance (^{13}C NMR) spectra were acquired using either Varian Mercury Plus 400 MHz or Bruker AVANCE 400 MHz spectrometers. All chemical shifts are reported in parts per

million and calibrated against the residual solvent signals of $CDCl_3$ (δ 7.24, 77.0 ppm). Coupling constants are indicated in Hertz (Hz). Multiplicities are reported as follows: s (singlet), d (doublet), t (triplet), q (quartet), m (multiplet), and br (broad). Melting points were measured using a Fargo MP-1D melting point apparatus without correction. Infrared spectra were recorded on Varian 640-IR spectrometer. Mass spectra with an electrospray ionization (ESI) system or a fast atom bombardment (FAB) system were determined on WATERS LCT Premier Xe spectrometer and JMS-700 double focusing mass spectrometer, respectively. UV-visible absorption spectra were recorded at 25 ^{o}C using a Hewlett-Packard 8453A diode array spectrometer under the control of a Pentium PC running the manufacturer-supplied software package. Fluorescence spectra were recorded on a Hitachi F-4500 spectrofluorometer. The TEM images were acquired from Hitachi H-7650 and H-7100 transmission electron microscopes. The TEM specimen was prepared by settling a drop (10 μL) of micelle solution (0.25 mg/mL) onto 200-mesh carbon-coated copper grids for 15 min and then stained with 2% phosphotungstic acid for 10 sec followed by rinsing with deionized water twice prior to imaging. The cryo-TEM image was acquired from FEI Tecnai G2 F20 TWIN transmission electron microscope. The confocal laser scanning microscopy (CLSM) images were obtained from Leica TCS SP5 confocal microscope. The hydrodynamic diameters were obtained by dynamic light scattering measurement with Malvern Zetasizer Nano Particle Analyzer ZS. The absorbance values of cell viability assay were recorded using a Bio-Rad model 680 microplate reader. The molecular weights and polydispersities of the copolymers were determined by a Waters 1515 gel permeation chromatography (GPC) instrument equipped with Ultrahydrogel^{TM} 500 (7.8×300 mm) and a Waters 2414 refractive index detector. The measurements were performed using double distilled water as the eluent at a flow rate of 1 mL/min at 25 ℃ and a series of narrow polyethylene oxide (PEO) standards for calibration. The molecular weights of the copolymers were also determined by a Bruker Autoflex Speed MALDI-TOF/TOF mass spectrometer (Bruker Daltonics) equipped with a 355 nm Nd:YAG

laser. Mass spectra were obtained by averaging 3000 laser shots in reflectron mode. The MALDI sample was prepared by spotting a drop of polymer solution (0.4 μL) on MALDI plate first and allowed to dry followed by the addition of 0.4 μL 2,5-dihydroxybenzoic acid (DHB) matrix. Flow cytometry was performed with a BD FACSCanto II flow cytometer (BD Biosciences) and analyzed with Flowing Software (version 2.5.0, Turku Bioimaging).

2. Experimental procedures and physical data

2.1 Synthesis and characterization of TMC monomers used in this work

TMC monomers used in this work were readily synthesized from their corresponding alcohols or amines by coupling with **TMC-COOH** or activated derivatives of **TMC-COOH** via esterification/amidation pathways, as shown in the Scheme 1b of the main manuscript. Chemical structures of all TMC monomers with the corresponding isolated yields were shown in Scheme S1. Most of alcohol or amine precursors for TMC monomers are commercially available or known compounds, except that of **TMC-O3dCHBE**, which required 3-step synthesis as depicted in Scheme S2.

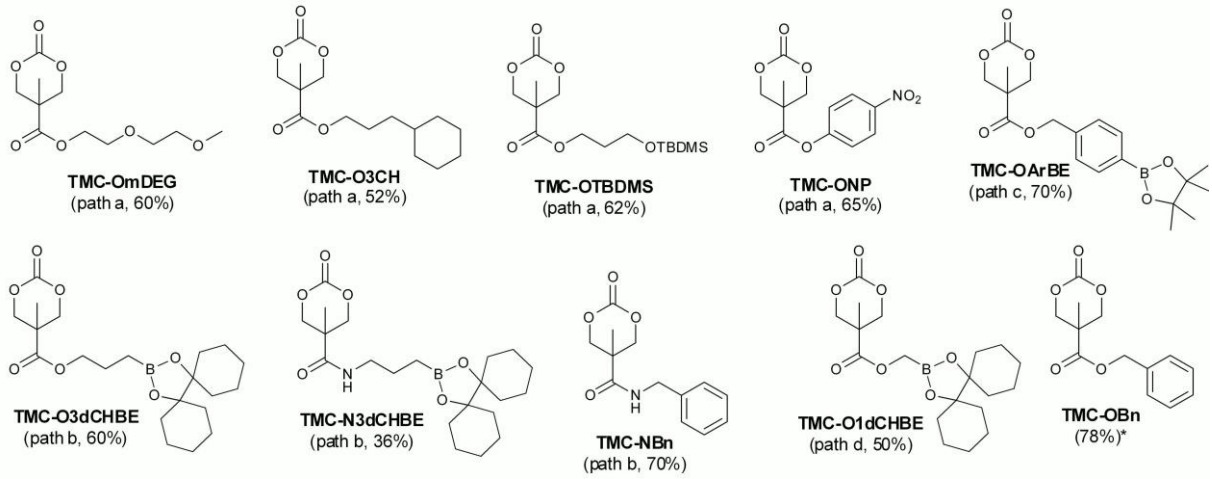

Scheme S1 Chemical structures of TMC monomers used in this work. The letters and numbers in the parentheses indicate the adopted synthetic pathways (referring to Scheme 1b in the main manuscript) and the corresponding isolated yields. ***TMC-OBn** is the precursor of common intermediate **TMC-COOH** and prepared from commercially available **bis-MPA** via benzylation followed by esterification.[1]

2.1.1 TMC-OmDEG and TMC-OArBE

2-(2-methoxyethoxy)ethyl 5-methyl-2-oxo-1,3-dioxane-5-carboxylate (TMC-OmDEG)[7] (path a)

Oxalyl chloride (5.6 mL, 67 mmol) was added to a solution of **TMC-COOH** (9.3 g, 58 mmol) in anhydrous THF (50 mL) with 3 drops of anhydrous DMF at room temperature, and the reaction mixture was stirred for 1 h under argon atmosphere. Volatiles were removed *in vacuo* to afford crude acid chloride, which was then charged in anhydrous THF (50 mL). A solution of diethylene glycol monomethyl ether (9.6 mL, 70 mmol) and triethylamine (7.7 mL, 70 mmol) in anhydrous THF was added dropwise into the reaction mixture in sequence, subsequently keeping stirring for 4 h at ambient temperature. The resulting white precipitate was filtered off and filtrate was concentrated under reduced pressure to provide crude product, which was further purified by flash column chromatography on silica gel with ethyl acetate-hexane (1:1) as an eluent to provide 9.1 g of **TMC-OmDEG** as colorless oil in 60 % isolated yield: TLC (ethyl acetate/hexane (3:1)) R_f = 0.3; ^{1}H NMR (400 MHz, $CDCl_3$) δ 4.66 (d, J = 10.8 Hz, 2H), 4.32 (t, J = 4.8 Hz, 2H), 4.17 (d, J = 10.8 Hz, 2H), 3.68-3.49 (m, 6H), 3.33 (s, 3H), 1.3 (s, 3H); ^{13}C NMR (100 MHz, $CDCl_3$) δ 171.0, 147.4, 72.9, 71.8, 70.4, 68.6, 64.8, 59.0, 40.1, 17.5; IR (neat) ν 2884, 1735, 1466, 1175, 767 cm^{-1}; ESI-HRMS: calcd for $C_{11}H_{19}O_7$ ($[M+H]^+$) 263.1129; found 263.1131.

[4-(tetramethyl-1,3,2-dioxaborolan-2-yl)phenyl]methyl 5-methyl-2-oxo-1,3-dioxane-5-carboxylate (TMC-OArBE) (path c)

A solution of diisopropyl azodicarboxylate (3 mL) in anhydrous THF (10 mL) was slowly added via addition funnel to a solution of **TMC-COOH** (1 g, 6.24 mmol), [4-(4,4,5,5-tetramethyl-1,3,2-dioxaborolan-2-yl)-phenyl]methanol (1.40 g, 5.98 mmol) and triphenylphosphine (1.63 g, 6.24 mmol) in anhydrous THF (25 mL) at room temperature. The reaction was allowed to stir for 4 h at room temperature and the solvent was evaporated *in*

vacuo to give a deep orange crude, which was further purified by flash column chromatography on silica gel with ethyl acetate-hexane (1:2 to 1:1) as an eluent followed by reprecipitation from diethyl ether to afford 1.47 g of **TMC-OArBE** as white solid in 70 % isolated yield: mp 85~90 ^{o}C; TLC (ethyl acetate/hexane (1:1)) R_f= 0.25; ^{1}H NMR (400 MHz, $CDCl_3$) δ 7.79 (d, *J* = 8 Hz, 2H), 7.30 (d, *J* = 8 Hz, 2H), 5.20 (s, 1H), 4.68 (d, *J* = 10.8 Hz, 2H), 1.32-1.30 (s, 15H); ^{11}B NMR (128 MHz, $CDCl_3$) δ 32.5; ^{13}C NMR (100 MHz, $CDCl_3$) δ 170.8, 147.4, 137.6, 135.2, 135.0, 127.4, 84.0, 72.9, 67.8, 40.2, 24.8, 17.6; IR (neat) *v* 3112, 2978, 1765, 1735, 1361, 858 cm^{-1}; ESI-HRMS: calcd for $C_{19}H_{26}BO_7$ ($[M+H]^+$) 337.1779; found 337.1772.

2.1.2 TMC-O3dCHBE

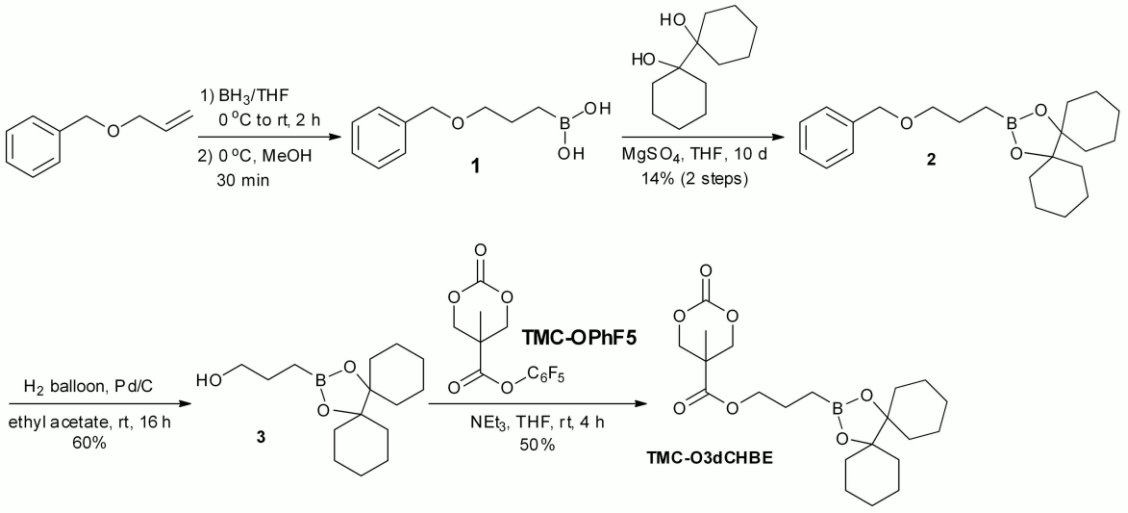

Scheme S2 A synthetic route to prepare 3-{13,15-dioxa-14-boradispiro[5.0.5^7.3^6]pentadecan-14-yl}propyl 5-methyl-2-oxo-1,3-dioxane-5-carboxylate (**TMC-O3dCHBE**)

14-[3-(benzyloxy)propyl]-13,15-dioxa-14-boradispiro[5.0.5^7.3^6]pentadecane (2)

A borane-tetrahydrofuran complex (1M, 172 mL, 172 mmol) was added dropwise into a solution of [(prop-2-en-1-yloxy)methyl]benzene[8] (25.49 g, 172 mmol) in anhydrous THF (250 mL) at 0 °C and then warmed up to room temperature within 2 h. The reaction mixture was then quenched by adding methanol dropwise at 0 °C over 30 min (CAUTION: hydrogen gas was evolved). Subsequently, water (20 mL) was added into the reaction mixture to convert the resulting dimethyl borate to the corresponding boronic acid. The resulting mixture was concentrated under the reduced pressure to give crude **1** as a colorless oil, which was taken up in THF (60 mL) without further purifications.

1-(1-Hydroxycyclohexyl)cyclohexan-1-ol[6] (6.12 g, 30.91 mmol) and excess equivalents of $MgSO_4$ were added to the aforementioned solution of **1** and then stirred at room temperature for 10 d. The insoluble salts was removed by filtration and the filtrate was evaporated *in vacuo* to give the residue, which was further purified by flash column chromatography on silica gel with ethyl acetate-hexane (1:3) as an eluent to give 1.5 g of **2** as a colorless oil in 14% isolated yield (two steps): TLC (ethyl acetate/hexane (1:3)) R_f= 0.5; ^{1}H NMR (400 MHz,

$CDCl_3$) δ 7.33-7.31 (m, 5H), 4.49 (s, 1H), 3.45 (t, *J* = 6.8 Hz, 2H), 1.74 (m, 2H), 1.69-1.54 (m, 14H), 1.26-1.14 (m, 6H), 0.83 (t, *J* = 6.8 Hz, 2H); ^{11}B NMR (128 MHz, $CDCl_3$) δ 32.5; ^{13}C NMR (100 MHz, $CDCl_3$) δ 138.8, 128.2, 128.1, 127.5, 127.3; IR (neat) *v* 3083, 2934, 2857, 1451, 1369; ESI-HRMS: calcd for $C_{22}H_{34}BO_3$ ($[M+H]^+$) 357.2597; found 357.2601.

3-{13,15-dioxa-14-boradispiro[5.0.5^7.3^6]pentadecan-14-yl}propan-1-ol (3)

A mixture of compound **2** (7.6 g, 21.2 mmol) and Pd/C (10% w/w, 0.76 g) in ethyl acetate (100 mL) was equipped with a hydrogen balloon, and the mixture was stirred at room temperature for 16 h. The whole mixture was filtered through Celite, and the filtrate was concentrated *in vacuo* to give a yellow crude residue, which was further purified by flash column chromatography on silica gel with ethyl acetate-hexane (1:3) as an eluent to give 3.4 g of **3** as a colorless oil in 60% isolated yield: TLC (ethyl acetate/hexane (1:3)) R_f = 0.5; ^{1}H NMR (400 MHz, $CDCl_3$) δ 3.61 (t, *J* = 6.4 Hz, 2H), 2.09 (s, 1H), 1.72-1.56 (m, 16H), 1.23-1.22 (m, 6H), 0.83 (t, *J* = 6.4 Hz, 2H); ^{11}B NMR (128 MHz, $CDCl_3$) δ 32.5; ^{13}C NMR (100 MHz, $CDCl_3$) δ 84.3, 64.9, 32.3, 30.6, 27.2, 25.6, 22.2; IR (neat) *v* 2935, 2860, 1449, 1369, 943 cm^{-1}; ESI-HRMS: calcd for $C_{15}H_{27}BNaO_3$ ($[M+Na]^+$) 289.1939; found 289.1948.

3-{13,15-dioxa-14-boradispiro[5.0.5^7.3^6]pentadecan-14-yl}propyl 5-methyl-2-oxo-1,3-dioxane-5-carboxylate (TMC-O3dCHBE) (path b)

To a solution of **TMC-OPhF5** (1.28 g, 3.93 mmol) and CsF (0.17 g, 1.10 mmol) in anhydrous THF (15 mL) was added slowly a solution of **3** (0.95 g, 3.57 mmol) in THF (10 mL) at room temperature and then the reaction mixture was stirred for 72 h at 50 ^{o}C. The solvent was removed under reduced pressure and then the residue was purified by flash column chromatography on silica gel with ethyl acetate-hexane (1:2) as an eluent to give 0.87 g of **TMC-O3dCHBE** as colorless oil in 60 % isolated yield: TLC (ethyl acetate/hexane (1:2)) R_f = 0.5; ^{1}H NMR (400 MHz, $CDCl_3$) δ 4.66 (d, *J* = 10.8 Hz, 2H), 4.18-4.15 (m, 4H), 1.79-

1.66 (m, 2H), 1.63-1.56 (m, 6H), 1.33 (s, 3H), 1.23-1.11 (m, 6H), 0.83 (t, J = 6.4 Hz, 2H); ^{11}B NMR (128 MHz, $CDCl_3$) δ 32.5; ^{13}C NMR (100 MHz, $CDCl_3$) δ 171.0, 147.5, 84.3, 73.0, 68.0, 40.1, 32.4, 25.6, 23.2, 22.2, 17.8; IR (neat) ν 2931, 2858, 1738, 1518, 1241, 995 cm^{-1}; ESI-HRMS: calcd for $C_{21}H_{34}BO_7$ ($[M+H]^+$) 409.2394; found 409.2398.

2.1.3 TMC-O1dCHBE, TMC-O3CH, TMC-OTBDMS, TMC-ONP and TMC-N3dCHBE

13,15-dioxa-14-boradispiro[5.0.5^7.3^6]pentadecan-14-ylmethyl 5-methyl-2-oxo-1,3-dioxane-5-carboxylate (TMC-O1dCHBE) (path d)

A solution of 14-(iodomethyl)-13,15-dioxa-14-boradispiro[5.0.5^7.3^6]pentadecane[6] (1.2 g, 4.67 mmol) in THF (35 mL) was added into a mixture of **TMC-COOH** (0.19 g, 1.17 mmol) and triethylamine (0.19 mL, 1.4 mmol) dissolved in anhydrous THF (12 mL) at room temperature. The reaction was allowed to stir for 4 h at room temperature and the solvent was evaporated *in vacuo* to give a yellow residue, which was further purified by flash column chromatography on silica gel with ethyl acetate-hexane (1:1) as an eluent followed by reprecipitation from cold diethyl ether to afford 0.22 g of **TMC-O1dCHBE** as a white solid in 50% isolated yield: mp 138~145 ^{o}C; TLC (ethyl acetate/hexane (1:1)) R_f = 0.3;^{1}H NMR (400 MHz, $CDCl_3$) δ 4.67 (d, *J* = 10.8 Hz, 2H), 4.19 (d, *J* = 10.8 Hz, 2H), 3.95 (s, 2H), 1.71-1.50 (m, 22H), 1.38 (s, 3H), 1.23-1.11 (m, 6H); ^{11}B NMR (128 MHz, $CDCl_3$) δ 32.5; ^{13}C NMR (100 MHz, $CDCl_3$) δ 171.5, 147.4, 85.6, 73.0, 39.8, 32.2, 25.4, 22.1, 17.9; IR (neat) *v* 2929, 2858, 1761, 1731, 1174 cm^{-1}; ESI-HRMS: calcd for $C_{19}H_{30}BO_7$ ($[M+H]^+$) 381.2088; found 381.2085.

3-cyclohexylpropyl 5-methyl-2-oxo-1,3-dioxane-5-carboxylate (TMC-O3CH)

The procedure used for the synthesis of **TMC-O3CH** is similar to that used for **TMC-OmDEG** (path a), and was performed on a 5.8 mmol scale by using 3-cyclohexylpropan-1-ol to replace diethylene glycol monomethyl ether, and gave **TMC-O3CH** as a colorless oil (0.86 g, 3.03 mmol, 52% yield): TLC (ethyl acetate/hexane (1:1)) R_f = 0.3; ^{1}H NMR (400 MHz, $CDCl_3$) δ 4.66 (d, *J* = 10.8 Hz, 2H), 4.16 (m, 4H), 1.69-1.59 (m, 7H), 1.32 (s, 3H), 1.21-1.16 (m, 6H), 0.86 (m, 2H); ^{13}C NMR (100 MHz, $CDCl_3$) δ 171.1, 147.4, 73.0, 66.7, 40.1, 37.2,

33.3, 33.2, 26.5, 26.3, 25.8, 17.7; IR (neat) *v* 2922, 2850, 1765, 1466, 1176 cm^{-1}; ESI-HRMS: calcd for $C_{15}H_{25}O_5$ ($[M+H]^+$) 285.1704; found 285.1702.

3-[(tert-butyldimethylsilyl)oxy]propyl 5-methyl-2-oxo-1,3-dioxane-5-carboxylate (TMC-OTBDMS)

The procedure used for the synthesis of **TMC-OTBDMS** is similar to that used for **TMC-OmDEG** (path a), and was performed on a 5.8 mmol scale by using 3-[(*tert*-butyldimethylsilyl)oxy]propan-1-ol[5] to replace diethylene glycol monomethyl ether, and gave **TMC-OTBDMS** as a colorless oil (1.19 g, 3.58 mmol, 62% yield): TLC (ethyl acetate/hexane (1:1)) R_f= 0.3; ^{1}H NMR (400 MHz, $CDCl_3$) δ 4.65 (d, *J* = 10.8 Hz, 2H), 4.28 (t, *J* = 6.4 Hz, 2H), 4.17 (d, *J* = 10.8 Hz, 2H), 1.84 (t, *J* = 6.4 Hz, 2H), 1.3 (s, 3H), 0.86 (s, 9H), 0.02 (s, 6H); ^{13}C NMR (100 MHz, $CDCl_3$) δ 171.0, 147.4, 73.0, 63.3, 59.0, 40.1, 31.6, 25.8, 18.2, 17.6; IR (neat) *v* 2955, 2930, 2857, 1767, 1468, 1101, 837 cm^{-1}; ESI-HRMS: calcd for $C_{15}H_{29}O_6Si$ ($[M+H]^+$) 333.1735; found 333.1733.

4-nitrophenyl 5-methyl-2-oxo-1,3-dioxane-5-carboxylate (TMC-ONP)

The procedure used for the synthesis of **TMC-ONP** is similar to that used for **TMC-OmDEG** (path a), and was performed on a 5.8 mmol scale by using nitrophenol to replace diethylene glycol monomethyl ether, and gave **TMC-ONP** as a yellow solid (1.05 g, 3.74 mmol, 65% yield): mp 146~149 ^{o}C; ^{1}H NMR (400 MHz, $CDCl_3$) δ 8.27 (d, *J* = 8.8 Hz, 2H), 7.28 (d, *J* = 8.8 Hz, 2H), 4.82 (d, *J* = 10.8 Hz, 2H), 4.32 (d, *J* = 10.8 Hz, 2H), 1.48 (s, 3H); ^{13}C NMR (100 MHz, $CDCl_3$) δ 169.2, 154.4, 147.1, 145.9, 125.4, 122.2, 72.7, 41.1, 17.3; IR (neat) *v* 2997, 1745, 1617, 1524, 1098 cm^{-1}; FAB-HRMS: calcd for $C_{12}H_{12}NO_7$ ($[M+H]^+$) 282.0614; found 282.0605.

***N*-(3-{13,15-dioxa-14-boradispiro[5.0.5^7.3^6]pentadecan-14-yl}propyl)-5-methyl-2-oxo-1,3-dioxane-5-carboxamide (TMC-N3dCHBE)**

The procedure used for the synthesis of **TMC-N3dCHBE** is similar to that used for **TMC-O3dCHBE** (path b), and was performed on a 6.8 mmol scale by using 3-{13,15-dioxa-14-boradispiro[5.0.5^7.3^6]pentadecan-14-yl}propan-1-amine[9] to replace 3-{13,15-dioxa-14-boradispiro[5.0.5^7.3^6]pentadecan-14-yl}propan-1-ol, and gave **TMC-N3dCHBE** as a white solid (0.99 g, 2.43 mmol, 36% yield): mp 125~126 ^{o}C; TLC (ethyl acetate/hexane (1:1)) R_f= 0.3; ^{1}H NMR (400 MHz, $CDCl_3$) δ 6.18 (s, 1H), 4.66 (d, J = 10.8 Hz, 2H), 4.19 (d, J = 10.8 Hz, 2H), 3.27 (m, 2H), 1.66-1.57 (m, 18H), 1.34 (s, 3H), 1.24-1.10 (m, 6H), 0.77 (t, J = 7.2 Hz, 2H); ^{11}B NMR (128 MHz, $CDCl_3$) δ 32.5; ^{13}C NMR (100 MHz, $CDCl_3$) δ 169.8, 147.6, 84.6, 74.2, 42.3, 40.2, 32.8, 31.0, 26.2, 26.0, 24.1, 22.7, 22.2, 18.3; IR (neat) ν 3082, 2935, 2859, 1750, 1650, 1543, 1370, 942 cm^{-1}; ESI-HRMS: calcd for $C_{21}H_{35}BNO_6$ ($[M+H]^+$) 408.2562; found 408.2557.

Benzyl 5-methyl-2-oxo-1,3-dioxane-5-carboxylate (TMC-OBn)[1] and ***N*-benzyl-5-methyl-2-oxo-1,3-dioxane-5-carboxamide (TMC-NBn)**[2] are known compounds and synthesized by using readily available literature procedures.

2.2 Synthesis and characterization of fluorescent initiator bis-MPA-3HF

3-hydroxy-*N*-{2-[4-(3-hydroxy-4-oxo-4H-chromen-2-yl)phenoxy]ethyl}-2-(hydroxylmethyl)-2-methylpropanamide (bis-MPA-3HF)

A mixture of **bis-MPA** (0.16 g, 1.17 mmol), **3-HFNH$_2$** (0.35 g, 1.17 mmol),[3] EDCI (0.34 g, 1.76 mmol), HOBt (0.11 g, 0.82 mmol) and DMAP (0.04 g, 0.35 mmol) were dissolved in chloroform (5 mL) at ambient temperature. DMF (5 mL) was then added into the reaction mixture until a homogenous solution was formed. After stirring at room temperature for 6 h, the reaction mixture was poured into water (50 mL) and extracted with ether (3 × 5 mL). The combined organic layers were dried over $MgSO_4$, filtered, and concentrated under reduced pressure to provide crude product, which was further purified by recrystallized from dichloromethane to afford 430 mg of **bis-MPA-3HF** as light yellow solid in 89 % isolated yield: mp 182~186 ^oC; TLC (ethyl acetate/hexane (1:1)) R_f= 0.2; ^1H NMR (400 MHz, $CDCl_3$) δ 8.18-8.22 (m, 3H), 7.67 (7.6Hz, 1H), 7.55 (d, *J* = 8.8 Hz, 1H), 7.38 (t, *J* = 7.6 Hz, 1H), 7.35 (s, 1H), 7.02 (d, *J* = 8.8 Hz, 2H), 7.01 (s, 1H), 4.14 (t, *J* = 5.2 Hz, 2H), 3.69-3.79 (m, 6H), 2.97 (s, 2H), 1.093 (s, 3H); ^{13}C NMR (100 MHz, $CDCl_3$) δ 177.2, 173.3, 160.1, 155.2, 145.6, 133.4, 129.6, 125.3, 124.5, 124.0, 120.8, 118.1, 114.6, 67.2, 66.7, 47.8, 38.7, 17.7; IR (neat) *v* 3303, 2937, 2877, 1600, 1555, 1253, 728 cm^{-1}; ESI-HRMS: calcd for $C_{22}H_{24}NO_7$ ($[M+H]^+$) 414.1551; found 414.1553.

2.3 Scope and limitation of organocatalytic ROP

The monomer scope of **TU**/**DBU** organocatalysts system was screened using **bis-MPA-3HF** diol as initiator and the results were summarized in Table S1.

As shown in entry 1~12 of Table S1 and discussed in the main manuscript, the monomers bearing a sterically bulky group near the cyclic carbonate functional group can't proceed ROP smoothly owing to the sterics of the monomer impeding the approachability toward the initiator or propagating alcohols. In addition, the screening results reveal that the **TU**/**DBU** activation for ROP is also highly susceptible to the electronic nature of monomers. Preparation of homopolymers by using activated ester-bearing TMC monomers **TMC-OPhF5** or **TMC-ONP** to give the corresponding polycarbonates, which can potentially convert to a variety of functional polycarbonates via post-polymerization modification (PPM) approach, was attempted by using **TU**/**DBU** as a catalyst (entry 13 and 14, respectively) but failed to afford the desired polycarbonates. Presumably, the incompatibility of **TMC-OPhF5** and **TMC-ONP** with **TU**/**DBU** for ROP can be attributed to that the **DBU**-activated nucleophiles (initiator or the propagating alcohols) preferentially attack the highly active pentafluorophenyl esters or nitrophenyl esters rather than six-membered cyclic carbonates. Recent report showed that the homopolymer of **TMC-OPhF5** can be achieved successfully by using acidic catalyst such as trifluoromethanesulfonic acid.[10]

On the other hand, amide linkage-bearing TMC monomers **TMC-N3dCHBE** (entry 15) and **TMC-NBn** (entry 16) displayed completely different reactivities toward **TU**/**DBU** system as compared to their ester counterparts, i.e. **TMC-O3dCHBE** and **TMC-OBn**. The reactivity disparity can be ascribed to the fact that the amide linkages interfere with the coordination between **TU** and cyclic carbonate moiety resulting in the sluggishness of ROP, as evidenced from the chemical shift at 3.3 ppm corresponding to the methylene protons next to the amide bond of **TMC-N3dCHBE** shifting to 3.9 ppm after mixed with **TU**.

Table S1 Scope and limitation of organocatalytic ROP for TMC monomers

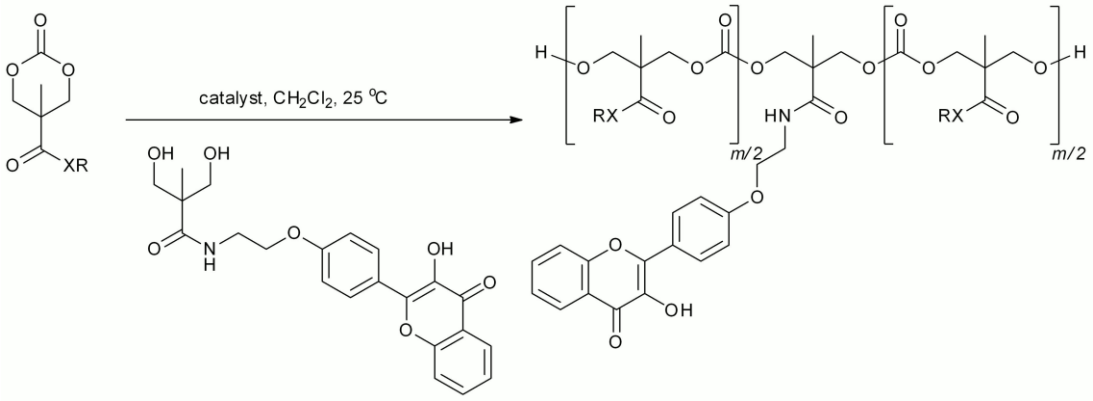

Entry	Monomer[a)]	Catalyst[b)]	Time [h]	Conversion[c)] [%]
1	**TMC-O3dCHBE**	TU-DBU	1.5	53
2	**TMC-O3dCHBE**	TU-DBU	3	95
3	**TMC-OArBE**	TU-DBU	3	70
4	**TMC-OmDEG**	TU-DBU	1.5	97
5	**TMC-O3CH**	TU-DBU	1.5	93
6	**TMC-OBn**	TU-DBU	1.5	98
7	**TMC-OTBDMS**	TU-DBU	1.5	97
8	**TMC-O1dCHBE**	TU-DBU	24	0
9	**TMC-O1dCHBE**	CH_3SO_3H	24	0
10	**TMC-O1dCHBE**	DMAP	24	0
11	**TMC-O1dCHBE**	TBD[d)]	24	0
12	**TMC-O1dCHBE**	$Sn(Oct)_2$	24	0
13	**TMC-OPhF5**	TU-DBU	1.5	0
14	**TMC-ONP**	TU-DBU	1.5	0
15	**TMC-N3dCHBE**	TU-DBU	24	0
16	**TMC-NBn**	TU-DBU	24	0

[a)]Condition: 0.1 M monomer in anhydrous CH_2Cl_2 with 0.002 M **bis-MPA-3HF** initiator, 25 °C; [b)]TU-DBU: both 5 mol%; CH_3SO_3H: 1 mol%; DMAP: 5 mol%; TBD: 5 mol%; $Sn(Oct)_2$: 0.34 mol%; [c)]Determined by ^{1}H NMR spectroscopy; [d)]TBD: 1,5,7-Triazabicyclo[4.4.0]dec-5-ene.

2.4 Sequential synthesis of amphiphilic triblock copolymers by 3-hydroxyflavone-initiated ROP

2.4.1 HP-3HF-Alk$_3$PC and HP-3HF-ArPC triblock copolymers

Schematic illustration for sequential synthesis of two H_2O_2-reactive amphiphilic triblock copolymers H**P-3HF-Alk$_3$PC** and **HP-3HF-ArPC** is shown in Scheme 2 of the main manuscript. Detailed synthetic procedures are described as follow: **TMC-O3dCHBE** (0.2 mmol), **bis-MPA-3HF** (0.004 mmol) and **TU** (0.02 mmol) were charged into a 10 mL round bottom flask and dissolved in anhydrous dichloromethane (1.5 mL) at ambient temperature. A solution of **DBU** (0.02 mmol) in dichloromethane (0.5 mL) was then added into the reaction mixture in one portion to initiate ring-opening polymerization. At predetermined time intervals, a small aliquot of reaction solution was taken to determine the polymerization conversion by ^{1}H NMR spectroscopy. When the polymerization conversion reached >90%, the ROP was temporarily ceased by evaporating **DBU** catalyst and solvent. Subsequently, the reaction residue as the macroinitiator was redissolved into anhydrous dichloromethane (1.5 mL) and a solution of **TMC-OmDEG** (0.6 mmol), **TU** (0.02 mmol) and **DBU** (0.02 mmol) in dichloromethane (0.5 mL) were added to restart the 2nd-stage ring-opening polymerization under argon atmosphere. After the depletion of **TMC-OmDEG** monomer (conversion >90 %) monitored by ^{1}H NMR spectroscopy, the copolymerization was quenched by adjusting the pH to 6 with benzoic acid (4~5 mg), as indicated by the solution color from golden yellow (deprotonated 3-HF dye) to pale yellow (neutralized 3-HF dye). To remove unreacted monomers and residual catalysts, the reaction mixture was evaporated and the residue was purified by size exclusion chromatography on Sephadex LH-20 gel with THF as an eluent. The desired fractions were evaporated to afford 160 mg of **HP-3HF-Alk$_3$PC** triblock copolymer as pale yellow film in 54 wt% yield. The procedure used for the synthesis of **HP-3HF-ArPC** triblock copolymer was similar to that used for **HP-3HF-Alk$_3$PC**, and gave **HP-3HF-ArPC** triblock copolymer as light green film in 58 wt% yield.

2.4.2 HP-3HF-Alk$_3$PC-ctrl and HP-3HF-ArPC-ctrl triblock copolymers

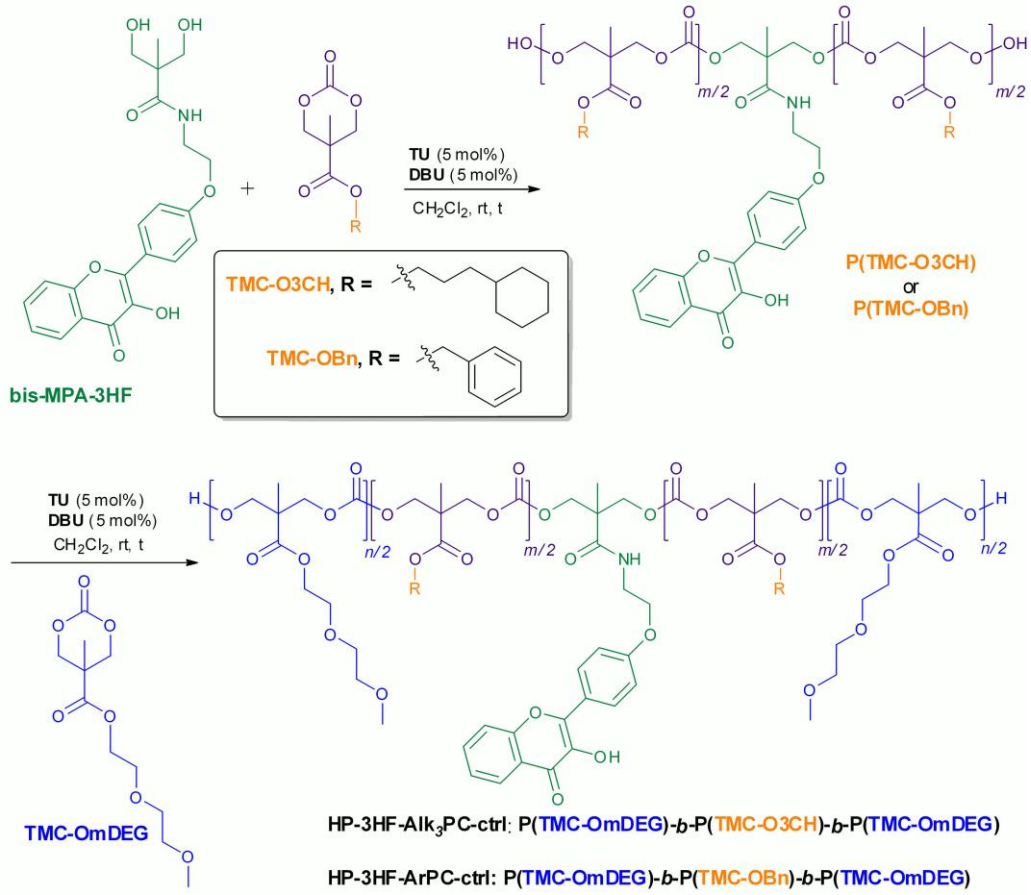

Scheme S3 Chemical structures and synthetic scheme of amphiphilic triblock polycarbonates for H_2O_2–inert **HP-3HF-Alk$_3$PC-ctrl** and **HP-3HF-ArPC-ctrl** micelles as controls of **HP-3HF-Alk$_3$PC** and **HP-3HF-ArPC**, respectively.

The procedures used for the synthesis of **HP-3HF-Alk$_3$PC-ctrl** and **HP-3HF-ArPC-ctrl** are similar to those used for the preparation of **HP-3HF-Alk$_3$PC** described in Section 2.4.1. **TMC-O3CH** or **TMC-OBn** instead of **TMC-O3dCHBE** was used as a monomer to afford the corresponding triblock copolymer as light green film in 69 and 71 wt% yield, respectively. (Scheme S3)

2.4.3 Synthesis of P(TMC-OmDEG)-*b*-P(TMC-O3OH)-*b*-P(TMC-OmDEG) as a control for products of H_2O_2-treated HP-3HF-Alk$_3$PC

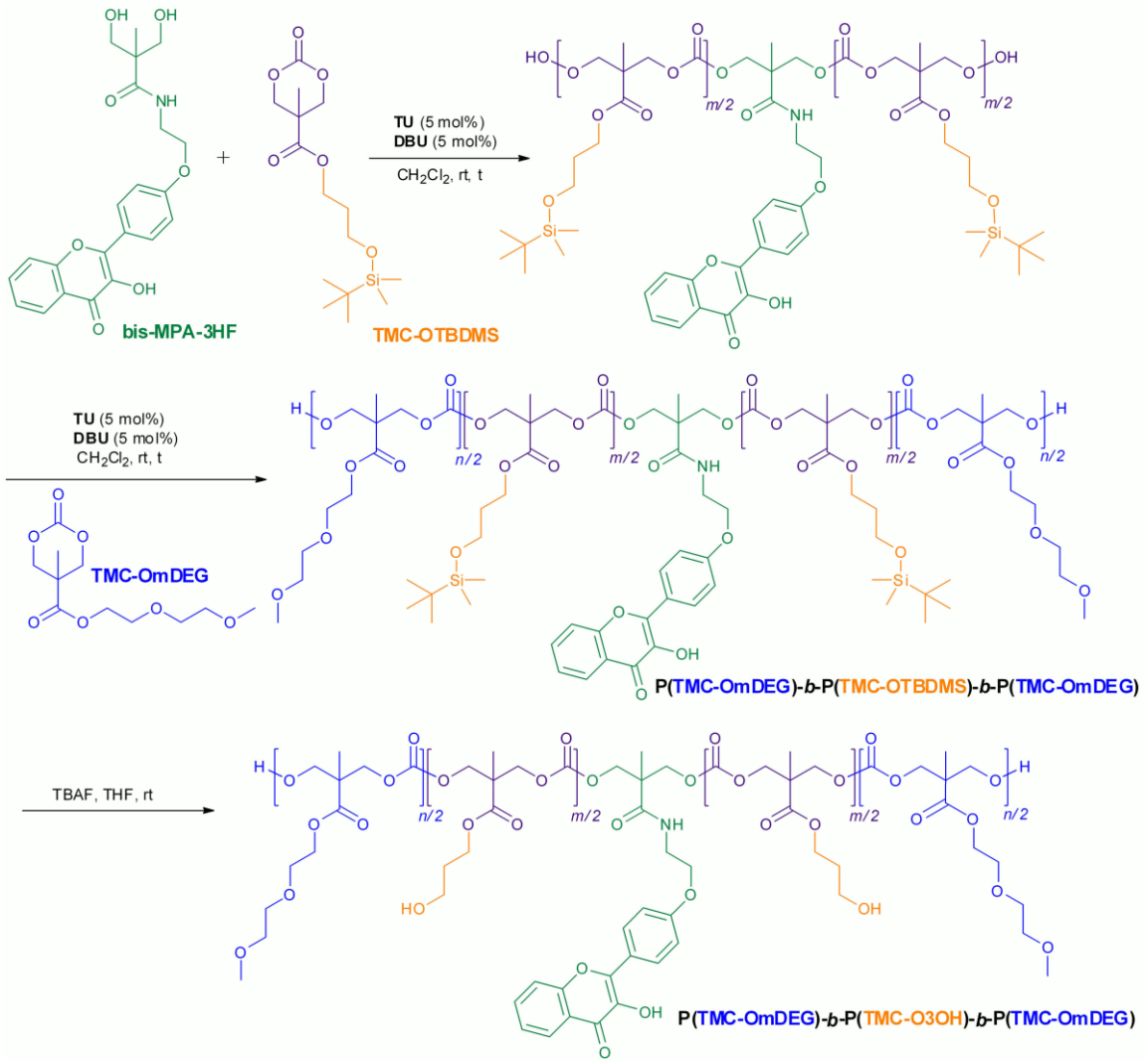

Scheme S4 Synthetic scheme of **P(TMC-OmDEG)-*b*-P(TMC-O3OH)-*b*-P(TMC-OmDEG)**

The procedure used for the synthesis of **P(TMC-OmDEG)-*b*-P(TMC-OTBDMS)-*b*-P(TMC-OmDEG)** triblock copolymer was similar to that used for **HP-3HF-Alk$_3$PC** described in Section 2.4.1. The polymerization was performed on a 0.8 mmol scale by using **TMC-OTBDMS** instead of **TMC-O3dCHBE** to afford the corresponding triblock copolymer as a light green film in 95 wt% yield. Subsequently, a solution of tetra-*n*-butylammonium fluoride in THF (1M, 1 mL, 1 mmol) was added in one portion into a solution of **P(TMC-OmDEG)-*b*-P(TMC-OTBDMS)-*b*-P(TMC-OmDEG)** triblock copolymer dissolved in THF

(2 mL) at room temperature and the resulting reaction mixture was allowed to stir for 18 h. After the deprotection of **OTBDMS** moieties, monitored by ^{1}H NMR spectroscopy, the reaction solvent was evaporated and the residue was purified by size exclusion chromatography on Sephadex LH-20 gel with THF as an eluent. The desired fractions were collected and evaporated to afford **P(TMC-OmDEG)-*b*-P(TMC-O3OH)-*b*-P(TMC-OmDEG)** triblock copolymer as a robin's egg blue film in 60 wt% yield. (Scheme S4)

2.5 Preparation of HP-3HF-Alk$_3$PC and HP-3HF-ArPC micelles

A solution of **HP-3HF-Alk$_3$PC** triblock copolymer (500 mg) in DMSO (100 μL) was added dropwise into 10 mM aqueous HEPES buffer solution (1900 μL) under a stirring rate of 360 rpm. After stirring for 10 min, the resulting mixture was homogenized by sonication for another 10 min to furnish a colloid-like **HP-3HF-Alk$_3$PC** micelle solution. Accordingly, **HP-3HF-ArPC** micelle solution was also prepared from **HP-3HF-ArPC** triblock copolymer using the same procedure.

2.6 Preparation of Nile red-loaded HP-3HF-ArPC polymeric micelles (NR@HP-3HF-ArPC)

The Nile red-encapsulated micelles (**NR@HP-3HF-ArPC**) were prepared in an analogous manner described in the fabrication of **HP-3HF-ArPC** micelles. A solution of Nile red (5 μg) and **HP-3HF-ArPC** triblock copolymer (500 μg) in DMSO (100 μL) was added into aqueous HEPES buffer (pH 8) with gentle stirring followed by homogenization procedure as described above. The resulting Nile red-loaded micelle solution was further purified by dialysis for 24 h in deionized water so as to remove the unencapsulated Nile red fluorophores. The micelle solution was directly used for subsequent fluorescence experiments.

3. Characterization of amphiphilic triblock polycarbonates

3.1 Molecular weight characterization of amphiphilic triblock polycarbonates

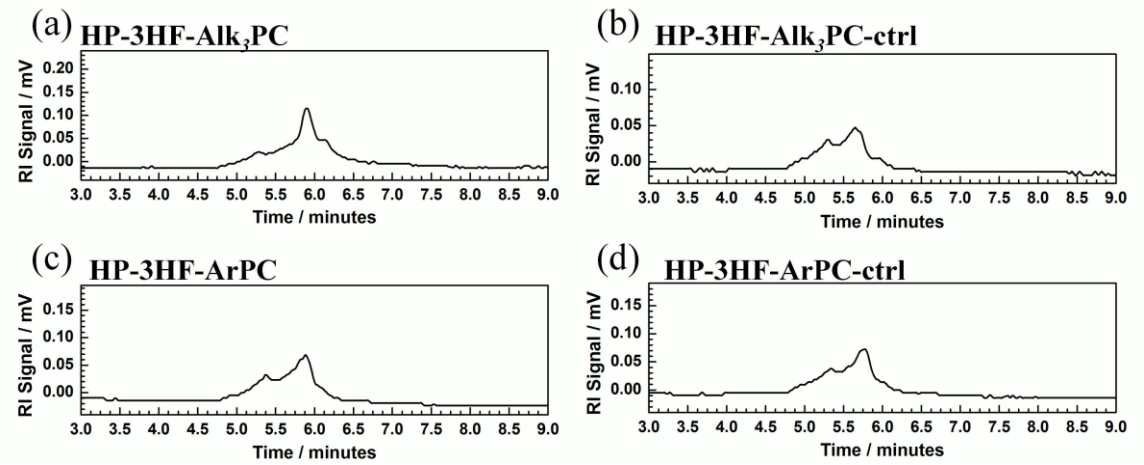

Fig. S1 GPC traces of amphiphilic triblock polycarbonates (a) **HP-3HF-Alk$_3$PC**, (b) **HP-3HF-Alk$_3$PC-ctrl**, (c) **HP-3HF-ArPC**, (d) **HP-3HF-ArPC-ctrl**, determined by GPC equipped with a refractive index detector in aqueous solution using polyethylene oxide (PEO) standards for calibration.

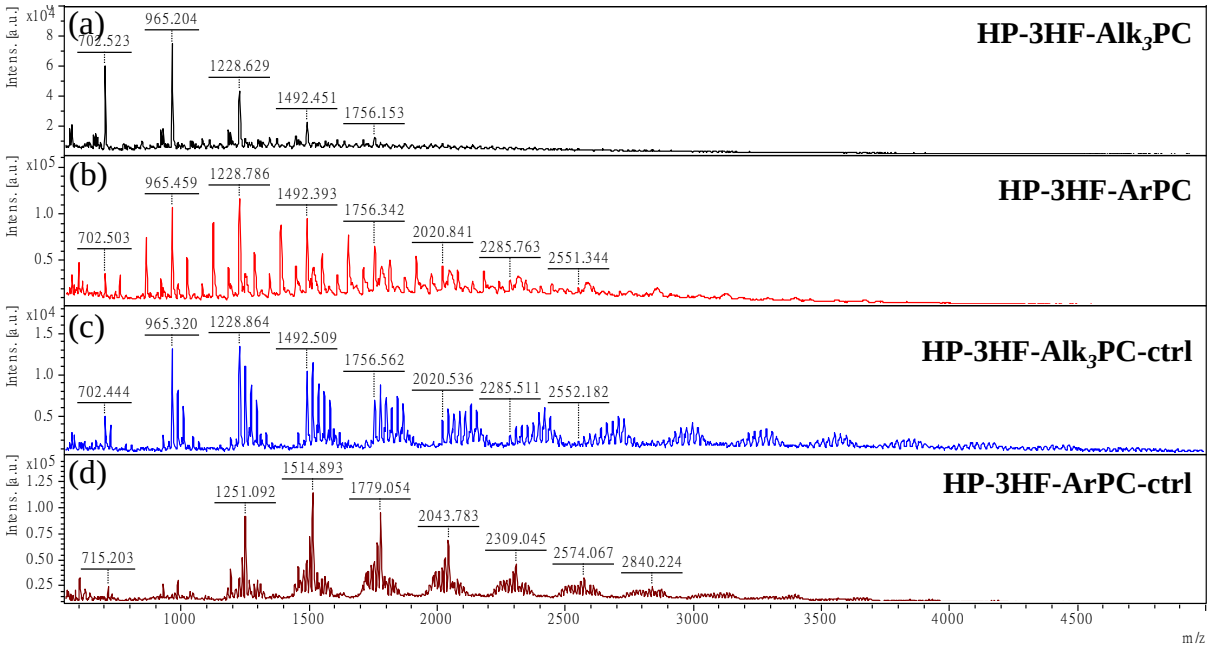

Fig. S2 MALDI-TOF/TOF spectra of amphiphilic triblock polycarbonates. (a) **HP-3HF-Alk$_3$PC**, (b) **HP-3HF-ArPC**, (c) **HP-3HF-Alk$_3$PC-ctrl**, (d) **HP-3HF-ArPC-ctrl** using 2,5-dihydroxybenzoic acid (DHB) as the matrix.

Table S2 Characterization of amphiphilic triblock polycarbonates with variable core-forming blocks

Copolymer	Yield[b] [wt%]	Composition[a] HB/HI/In		M_n [g/mol]				N_{ag}[f]	3-HF dyes	
		In feed	DP_{nmr}[c]	Theo.	NMR[c]	MALDI[d]	GPC_m[e]		Content[g] (per chain)	Q.Y[h]
HP-3HF-Alk$_3$PC	54	50/150/1	17/29/1	60342	15001	1756	328k	22	0.93	0.125
HP-3HF-ArPC	58	50/150/1	14/28/1	56739	12501	2551	406k	32	1.32	0.106
HP-3HF-Alk$_3$PC-ctrl	69	50/150/1	39/67/1	54139	29164	2552	670k	23	2.67	0.107
HP-3HF-ArPC-ctrl	71	50/150/1	47/135/1	52435	47735	2840	492k	10	2.30	0.143

[a]Composition HB/HI/In refers to the molar ratio of hydrophobic unit (HB) to hydrophilic unit (HI) to initiator (In) in a triblock copolymer chain; [b]Calculated by the weight of purified triblock copolymer divided by the total weight of the feed monomers and initiator; [c]Degree of polymerization (DP_{nmr}) and molecular weight were estimated by ^{1}H NMR spectroscopy using deuterated dichloromethane as solvent; [d]Determined by MALDI-TOF/TOF mass spectrometer equipped with a 355 nm Nd:YAG laser using 2,5-dihydroxybenzoic acid (DHB) as the matrix; [e]Determined by GPC equipped with refractive index detector in aqueous solution using polyethylene oxide (PEO) standards for calibration; [f]Aggregation number (N_{ag}) is defined as the number of polymer chains that assemble to form a micelle and given by dividing the molecular weight of one micelle ($M_{n,\ GPCm}$) by the molecular weight of one polymer chain ($M_{n,\ NMR}$); [g]Derived from the absorbance of copolymers in CH_2Cl_2 as compared to small molecular 3-HF dye 2-[4-(2-azidoethoxy)phenyl]-3-hydroxy-4H-chromen-4-one[3] in CH_2Cl_2 (ε = 28900 $M^{-1}cm^{-1}$ at 352 nm); [h]The FL quantum yields of the block copolymers were determined by comparing the luminescence with quinine sulfate (Q.Y. of quinine sulfate = 0.54) according to the established method.[11]

3.2 Structural analysis by ^{1}H NMR

A solution of **HP-3HF-Alk$_3$PC** (2.5 mg) in the co-solvents of THF (0.5 mL) and deionized water (9.5 mL) was treated with 200 mM H_2O_2 solution for 2 d at room temperature. The solvents were removed under reduced pressure and then the residue was charged in $CDCl_3$ for ^{1}H NMR analysis. For **HP-3HF-ArPC**, a solution of **HP-3HF-ArPC** (3.6 mg) in the co-solvents of THF (0.7 mL) and 10 mM K_2CO_3 aqueous solution (9.5 mL) was reacted with 100 mM H_2O_2 solution instead. Results of structural analysis by ^{1}H NMR are summarized in Fig. 4 of the main manuscript.

3.3 DLS measurements and TEM images

3.3.1 TEM images of **HP-3HF-Alk$_3$PC** and **HP-3HF-ArPC micelles before and after H_2O_2 treatment**

To monitor H_2O_2-triggered disintegration behaviors of micelles, time-dependent dynamic light scattering (DLS) measurements and transmission electron microscopy (TEM) before and after 250 mM H_2O_2 treatment of **HP-3HF-Alk$_3$PC** and **HP-3HF-ArPC** polycarbonates were conducted and analyzed, as shown in Fig. 5 of the main manuscript and Fig. S3, respectively. Both TEM images and DLS measurements of **HP-3HF-Alk$_3$PC** showed a substantial swelling after the extended treatment of H_2O_2 whereas that of **HP-3HF-ArPC** showed a complete disassembly to small fragments with a TEM image of debris clusters.

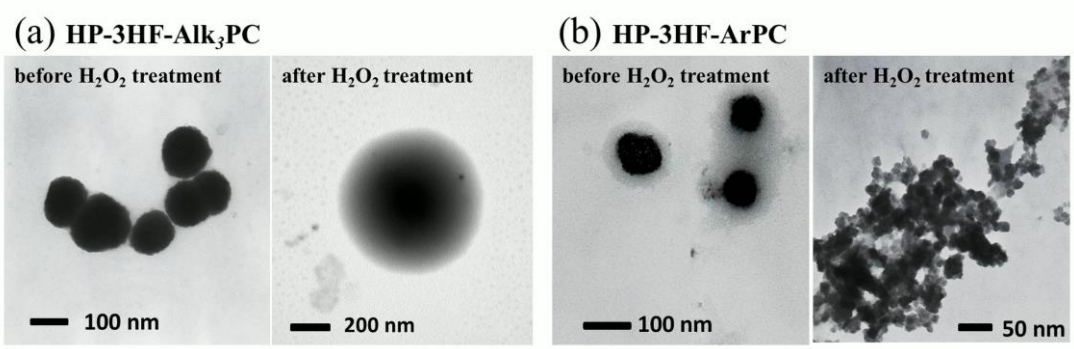

Fig. S3 TEM images of (a) **HP-3HF-Alk$_3$PC** and (b) **HP-3HF-ArPC** micelles before and after H_2O_2 treatment.

3.3.2 DLS measurements and TEM images of control micelles before and after H_2O_2 treatment

DLS measurements and TEM studies of control micelles **HP-3HF-Alk$_3$PC-ctrl** and **HP-3HF-ArPC-ctrl** before and after H_2O_2 treatment were conducted at the polymer concentration of 0.25 mg/mL and 250 mM H_2O_2. The corresponding DLS traces and TEM images were recorded at 0 and 48 h after the treatment of H_2O_2, and shown in Fig. S4. No significant difference in either sizes or shapes after H_2O_2 treatment was observed for both control micelles, showing their inertia toward H_2O_2.

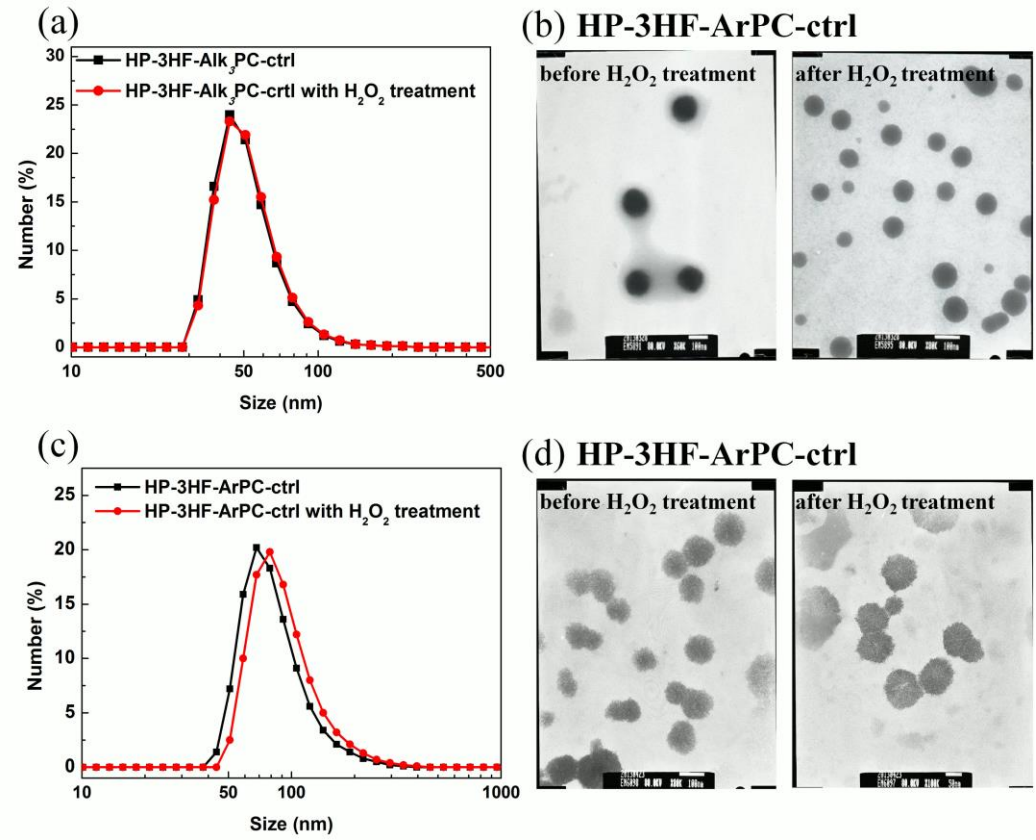

Fig. S4 (a) DLS measurements and (b) TEM images of control micelle **HP-3HF-Alk$_3$PC-ctrl** before and after H_2O_2 treatment. (c) DLS measurements and (d) TEM images of control micelle **HP-3HF-ArPC-ctrl** before and after H_2O_2 treatment.

3.4 Fluorescence measurements

Unless specifically mentioned, all the fluorescence studies were conducted at the micelle concentration of 0.25 mg/mL in a 10 mM aqueous HEPES (pH 7.4) buffer solution. The micelle solutions were excited at 356 nm and the emissions were collected from 375 to 670 nm, with 5-nm slits for both excitation and emission. Time-dependent fluorescence measurements of the micelles were conducted on the addition of 50 mM H_2O_2. Concentration-dependent fluorescence measurement of **HP-3HF-ArPC** was carried out in a 10 mM (pH 8.0) HEPES buffer solution.

3.4.1 Calculations of ESICT/ESIPT ratios for assessing the ratiometric effects

The data processing was performed as follows:[3] (1) The default wavelength-based fluorescence spectra was converted into wavenumber-based fluorescence spectra by running the manufacturer-supplied software package; (2) the intensities from 26.6 Kcm^{-1} to the middle wavevalley and from the middle wavevalley to 14.9 Kcm^{-1} were integrated as ESICT band energy and ESIPT band energy, respectively; (3) the ratios of integrated intensities were calculated by dividing ESICT band energy by ESIPT band energy; (4) the ratios were normalized by scaling the initial values to one. In all of time-dependent fluorescence experiments, the ratios of integrated intensities at t = 0 were scaled to one.

3.4.2 Time-dependent fluorescence measurements of HP-3HF-Alk$_3$PC and HP-3HF-ArPC micelles in the absence of H_2O_2

As control experiments, overlaid fluorescence spectra of **HP-3HF-Alk$_3$PC and HP-3HF-ArPC** micelles at various reaction times in the absence of H_2O_2 were shown in Fig. S5a and S5b, respectively. Correlations between reaction times and the normalized ratios of the integrated intensities of ESICT and ESIPT bands of the corresponding experiments are summarized in Fig. 6c of the main manuscript. No significant ratiometric variation was observed, validating H_2O_2 is indeed responsible for the ratiometric fluorescence transition. The normalized ratios of the ESICT and ESIPT are less than 2 over the entire reaction time for these two micelles in the absence of H_2O_2. A slight decrease in the fluorescence intensities of ESIPT bands of the two control micelles with time was observed, which may be attributed to the slow hydrolysis (degradation) of polycarbonate backbone in aqueous media leading to the partial soaking of 3-HF-containing micellar cores in water as well as the slight decrease of ESIPT bands. However, the ratiometric fluorescence change incurred by the spontaneous degradation of polycarbonates is relatively insignificant as compared to that generated by H_2O_2-induced disassembly or swelling. The phenomenon of degradation of polycarbonates in aqueous media also implicates the biodegradable nature of polycarbonates.

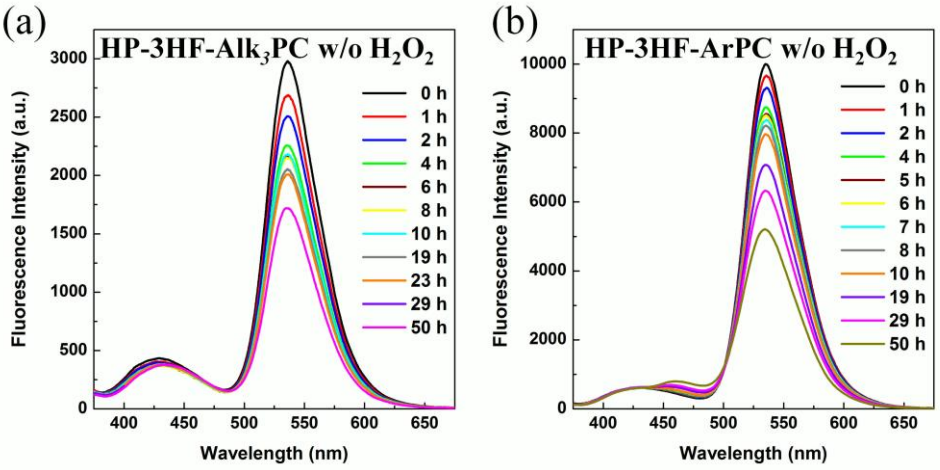

Fig. S5 Time-dependent fluorescence responses of (a) **HP-3HF-Alk$_3$PC** and (b) **HP-3HF-ArPC** micelles in the absence of H_2O_2.

3.4.3 Time-dependent fluorescence measurements of control micelles

At each experiment, an aliquot of H_2O_2 solution or water (for blank experiment) was added to **HP-3HF-Alk$_3$PC-ctrl** and **HP-3HF-ArPC-ctrl** micelles, respectively, at time = 0 and well mixed to give a final concentration of 50 or 0 (for blank) mM of H_2O_2. Fluorescence measurements of two control micelles at various reaction times without and with 50 mM H_2O_2 treatment were conducted, and the corresponding overlaid fluorescence spectra were shown in Fig. S6. No significant ratiometric fluorescence variation was observed in both control micelles whether the treatment of H_2O_2 or not, verifying the chemical inertia of **O3CH** and **OBn** core structures of **HP-3HF-Alk$_3$PC-ctrl** and **HP-3HF-ArPC-ctrl** micelles, respectively, toward H_2O_2. The phenomenon of degradation of polycarbonates in aqueous media leading to slight reduction of ESIPT bands was also observed in both control micelles.

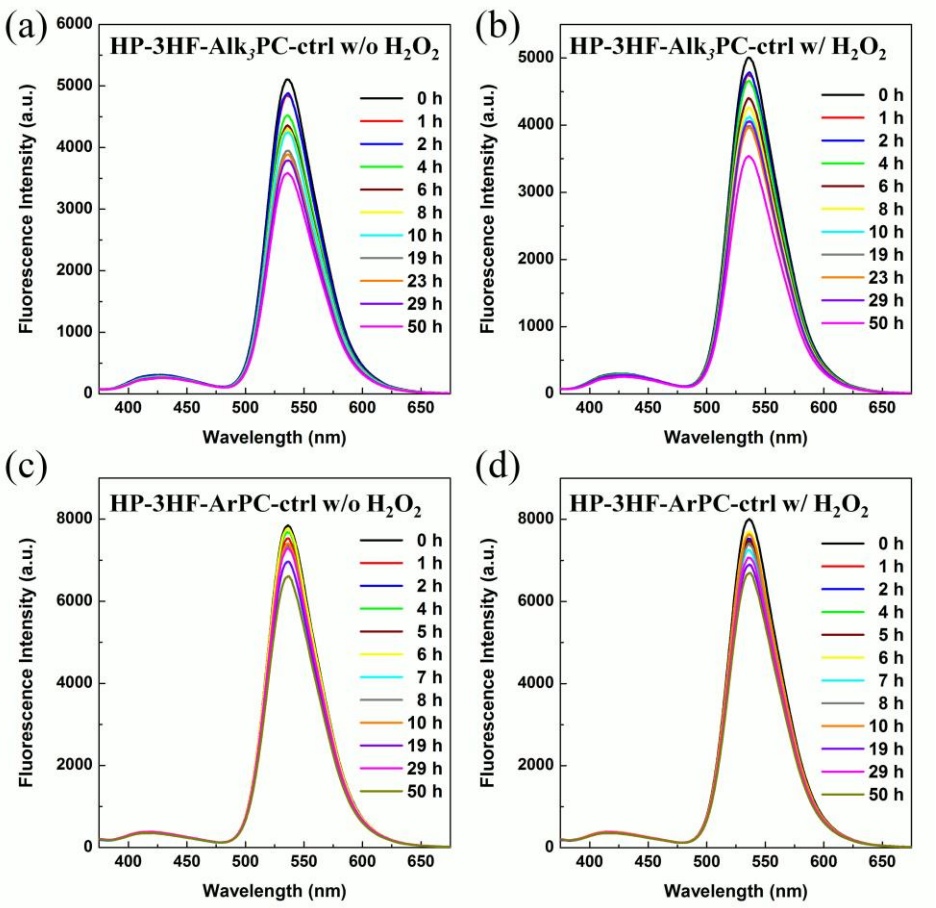

Fig. S6 Time-dependent fluorescence responses of control micelles **HP-3HF-Alk$_3$PC-ctrl** and **HP-3HF-ArPC-ctrl** in the presence or absence of 50 mM H_2O_2. (a) **HP-3HF-Alk$_3$PC-ctrl** without H_2O_2; (b) **HP-3HF-Alk$_3$PC-ctrl** with H_2O_2; (c) **HP-3HF-ArPC-ctrl** without H_2O_2; (b) **HP-3HF-ArPC-ctrl** with H_2O_2.

3.4.4 H_2O_2-dependent fluorescence measurements of HP-3HF-Alk$_3$PC and HP-3HF-ArPC micelles

H_2O_2-dependent fluorescence measurements of **HP-3HF-Alk$_3$PC** and **HP-3HF-ArPC** micelles were conducted at the polymer concentration of 0.25 mg/mL and various amounts of H_2O_2 ranging from 0 to 250 mM. Fluorescence spectra were recorded at 48 h after the addition of H_2O_2. The overlaid fluorescence spectra of **HP-3HF-Alk$_3$PC** and **HP-3HF-ArPC** micelles with various concentrations of H_2O_2 were shown in Fig. S7a and S7b. Corresponding fluorescent photoimages shown in Fig. S7c and S7d, respectively, at various concentrations of H_2O_2 display that **HP-3HF-Alk$_3$PC** and **HP-3HF-ArPC** micelles possess different sensing ranges for H_2O_2 and **HP-3HF-ArPC** is more sensitive than **HP-3HF-Alk$_3$PC**.

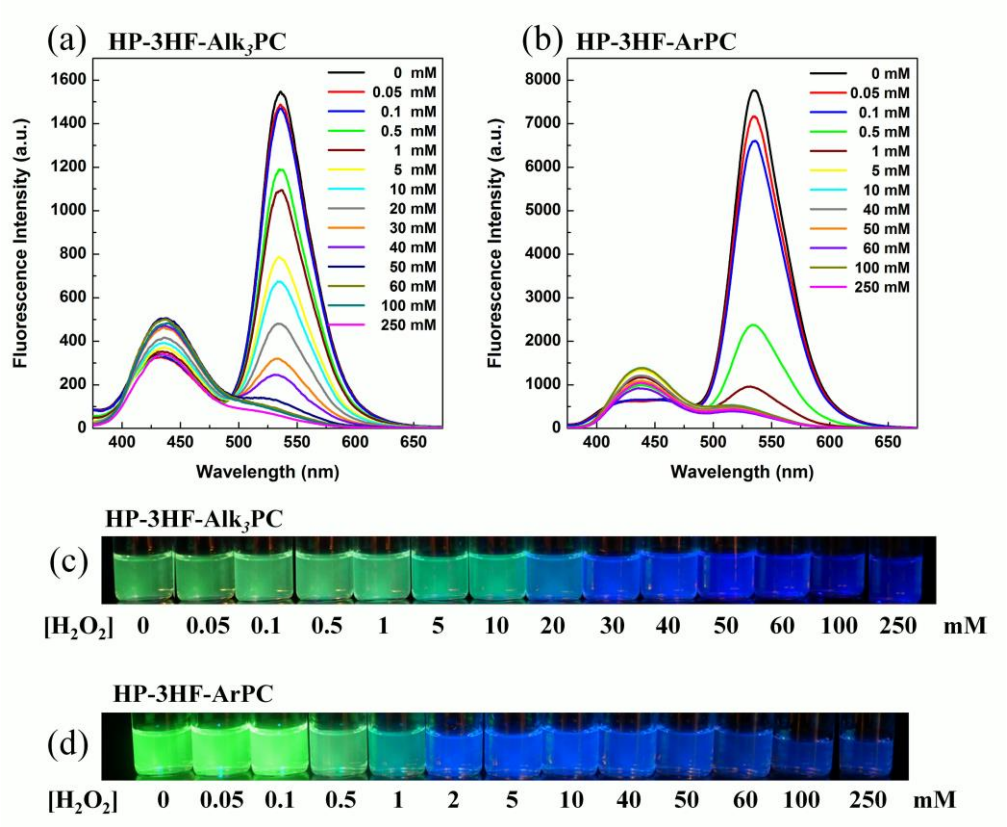

Fig. S7 Fluorescence responses of (a) **HP-3HF-Alk$_3$PC** and (b) **HP-3HF-ArPC** at various concentrations of H_2O_2. Corresponding photoimages of (a) and (b) are shown in (c) and (d), respectively. The two micelles with different core-forming moieties exhibit different sensing ranges for H_2O_2.

3.4.5 Photophysical evaluation of FRET experiments using Nile red as a model drug

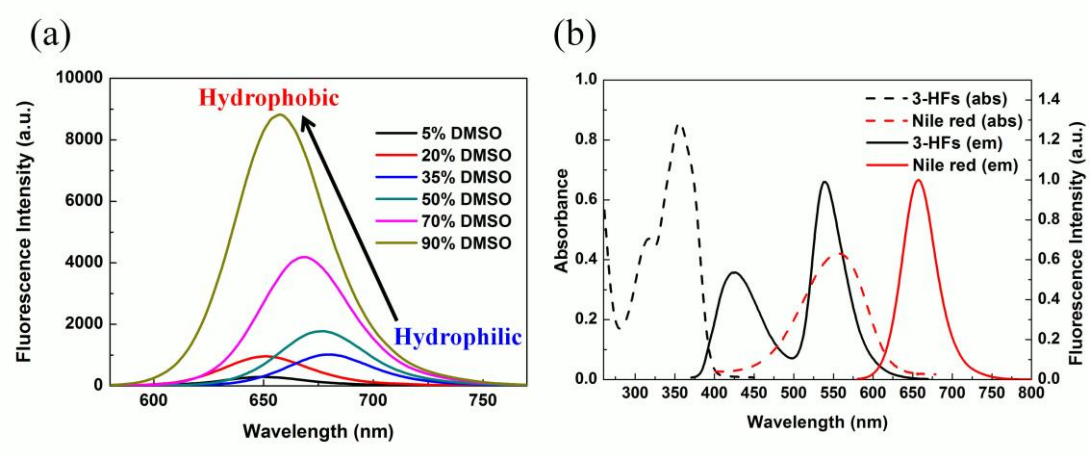

Fig. S8 Fluorescence properties of Nile red. (a) Overlaid fluorescence spectra of Nile red fluorophore (1×10^{-5} M) in various proportions of DMSO and water mimicking different hydrophilicity, which properly demonstrates the solvatochromic nature of Nile red. (b) Absorption and emission spectra of 3-HFs and Nile red at 1×10^{-5} M in 90% DMSO solution mimicking the hydrophobic environment of micellar cores. For clarity, emission spectra for 3-HFs and Nile red are normalized at 538 nm (ESIPT band) and 657 nm, respectively. The efficient overlap between ESIPT emission band of 3-HFs and absorption band of Nile red allows FRET between the two fluorophores feasible.

3.4.6 Release of Nile red from NR@HP-3HF-ArPC

The procedure used for time-dependent fluorescence measurement of **NR@HP-3HF-ArPC** in response to H_2O_2 was similar to that used for **HP-3HF-ArPC**. Briefly, **NR@HP-3HF-ArPC** (0.25 mg/mL) in a 10 mM aqueous pH 8.0 HEPES buffer solution was incubated with 2 mM H_2O_2 solution at 25 ^oC. The fluorescence spectra of **NR@HP-3HF-ArPC** solution were recorded at appropriate time points with excitation at 356 nm and emissions collected from 375 to 700 nm (5-nm slits for both excitation and emission).

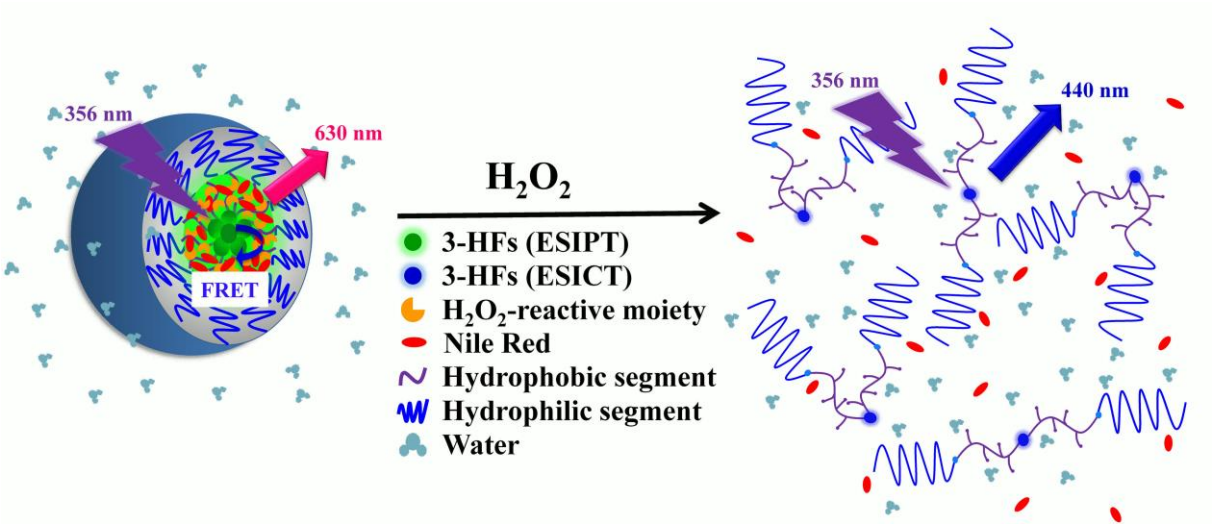

Fig. S9 Conceptual illustration of drug-loaded micellar nanoparticles and its drug release kinetics monitored by FRET fluorescence. Prior to H_2O_2 treatment, both 3-HFs and Nile red stay within the hydrophobic and confined core space, and the FRET occurs between the two fluorophores giving the red fluorescence of Nile red under the illumination of 356-nm light. The H_2O_2-triggered disassembly results in the leakage of Nile red from hydrophobic core to hydrophilic aqueous media and thus breaks the FRET pathway, finally giving the blue fluorescence (ESICT) of 3-HFs under the illustration of 356-nm light.

3.4.7 Proof for FRET between 3-HFs and Nile red in NR@HP-3HF-ArPC micelles

Evidence for donor absorption in the fluorescence excitation spectrum of the acceptor provides definitive proof for FRET. The fluorescence excitation spectrum of **NR@HP-3HF-ArPC** was thus measured from 250 to 675 nm by monitoring the fluorescence of Nile red (FRET acceptor) at 620 nm, as shown in Fig. S10. The fluorescence excitation spectrum of **NR@HP-3HF-ArPC** (Fig. S10) showing a small and broad excitation band at 330~400 nm, which exactly overlapped with the absorption band of 3-HF (FRET donor), proved that the FRET indeed occurs between 3-HF dye and Nile red in the core of **NR@HP-3HF-ArPC** micelle. The sharp excitation band that appeared at 310 nm is related to the second-order diffraction peak of grating (emission monitored at 620 nm). The broad excitation band at 500~600 nm is exactly the absorption (excitation) band of Nile red.

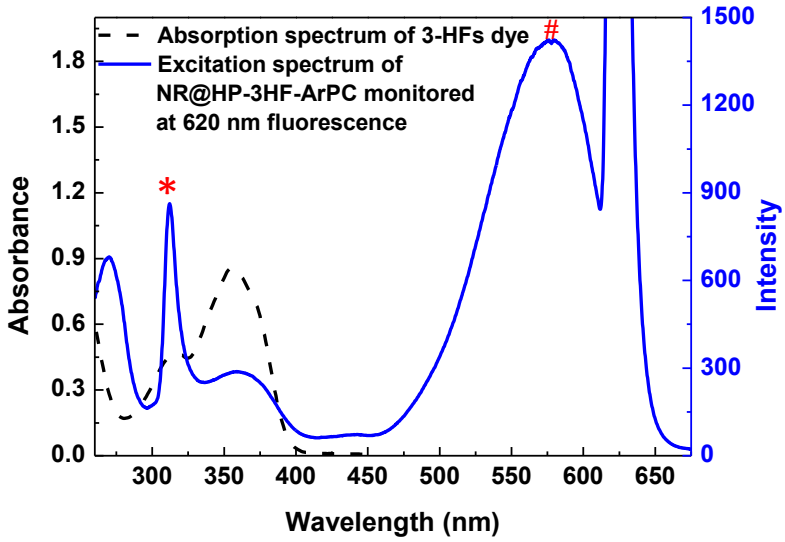

Fig. S10 Proof for FRET between 3-HFs and Nile red in **NR@HP-3HF-ArPC** micelles. Blue solid line: the fluorescence excitation spectrum of **NR@HP-3HF-ArPC** monitored at 620 nm fluorescence. Black dash line: the absorption spectrum of 3-HF dye. *: second-order diffraction peak of grating; #: the absorption (excitation) band of Nile red.

3.5 Cell experiments

3.5.1 Cell culture

RAW 264.7 murine macrophage cell lines were maintained in Dulbecco's modified eagles medium (DMEM) supplemented with 10 % heat-inactivated fetal bovine serum, 100 unit/mL penicillin, and 100 mg/mL streptomycin at 37 ^{o}C in a humidified and 5 % CO_2 atmosphere. After cell confluence reached 60~70%, the medium was removed and cells were washed once with PBS. Fresh complete DMEM medium was then added and RAW 264.7 cells were detached from the flask substrate by mechanically repeated pipetting or scraping. Cell suspension was centrifuged and the supernatant was aspirated. Cell pellets was then resuspend with appropriate aliquots of fresh complete DMEM medium and added into new culture vessels to allow for continued passaging. Cell counting can be conducted by using a hemocytometer with the assistance of trypan blue staining.

3.5.2 Cellular imaging

RAW 264.7 cells (1×10^5 cells/well) were seeded on coverslips in a 12-well plate and incubated at 37 ^{o}C, 5% CO_2 atmosphere overnight for cell adhesion. RAW 264.7 cells were washed once with PBS after removing DMEM medium, and treated with **HP-3HF-ArPC** micelle-containing DMEM medium (500 μg/mL) for 12 h. The **HP-3HF-ArPC**-containing medium was then removed and the cells were rinsed with serum-free DMEM and PBS once prior to fixation with 3.7% paraformaldehyde for 10 min at room temperature. Subsequently, cells were permeabilized in 0.5% Triton X-100 in PBS for 5 min and blocked with 1% BSA in PBS for 30 min followed by rinsing twice with PBS prior to CLSM observation. CLSM images were obtained on Leica TCS SP5 confocal microscope. Dual-colored emissions of **HP-3HF-ArPC** were acquired from 435~465 nm for ESICT and 535~565 nm for ESIPT, respectively, under irradiation of 405 nm diode laser.

3.5.3 Cell viability assay

The cytotoxicity of **HP-3HF-ArPC** polymeric micelles was evaluated using a 4-[3-(4-iodophenyl)-2-(4-nitrophenyl)-2H-5-tetrazolio]-1,3-benzene disulfonate (WST-1) assay. RAW 254.7 cells were seed at a density of 1×10^5 cell/mL in a 12-well plate and incubated for 24 h at 37 ^oC, 5 % CO_2 atmosphere prior to assay. Subsequently, RAW 254.7 cells were treated with fresh complete DMEM medium containing **HP-3HF-ArPC** micelles at various concentrations (0 to 500 μg/mL) for 24 h. The **HP-3HF-ArPC**-containing medium was then replaced with 10% WST-1 in complete DMEM medium and incubated for 2 h. After incubation, the resulting WST-1 solutions of each well were transferred into 96-well microplates to total volume of 200 μL/well. The absorbance at 450 nm was measured using a microplate reader and cell viability was calculated according to the following equation, where OD_{450} represents the optical density at 450 nm:

Cell viability = $[OD_{450}(sample)-OD_{450}(blank)]/[OD_{450}(control)-OD_{450}(blank)]$

3.5.4 Flow cytometry analysis

RAW 264.7 cells (2×10^5 cells) were seeded in 12-well plates (Corning® CellBIND®) and incubated at 37°C, 5% CO_2 atmosphere overnight for cell adhesion. After removing medium, cells were treated with fresh complete DMEM medium containing **HP-3HF-ArPC** micelles at various concentrations (0, 80, 160, 320 μg/mL) for another 12 h. After incubation, the cell cultures were rinsed once with PBS and RAW 264.7 cells were detached with 0.25% trypsin-EDTA medium (200 μL/well) at 37 ^oC for 8 min. After quenching the activity of trypsin by FBS-containing medium (800 μL/well), the cell suspension were aspirated and centrifuged (2200 rpm, 5 min) to afford cell pellets, which were re-suspend with a combination of PBS (50 μL) and 0.4% trypan blue solution (300 μL) and transferred to FACS tubes. The cells were stored on ice till the time of FACS analysis. Cells were then analyzed with 10,000 events acquired on a BD FACS Canto II instrument (BD Biosciences, USA) using the FSC,

SSC, ICT (Ex: 405 nm/Em: 450 ± 25 nm), IPT (Ex: 405 nm/Em: 585 ± 21 nm) channels. Cells without micelle treatment were used as controls. It is noteworthy that the fluorescence from non-internalized micelles on the surface of cells can be efficiently quenched by treating with trypan blue solution prior to flow cytometry analysis. The trypan blue treatment can efficiently rule out the signal misestimate originated from non-internalized micelles. The flow cytometry analysis (Fig. S11) indicated that the **HP-3HF-ArPC** micelles were indeed uptaken by RAW 264.7 cells. The fluorescence histograms of ICT and IPT channels in **HP-3HF-ArPC**-treated cells showed significant rightward shift as compared with untreated cells (controls). Furthermore, the gate populations of ICT-positve and IPT-positive cells increase with the concentration of micelles incubated.

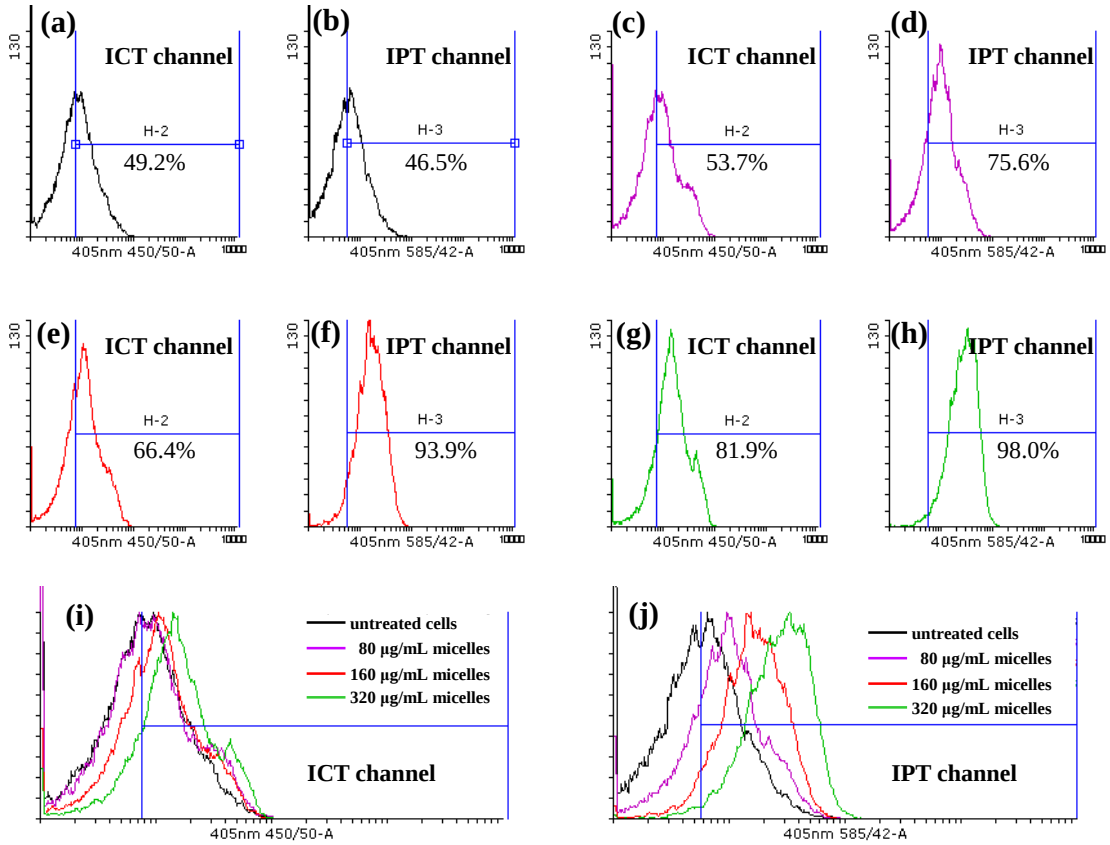

Fig. S11 Flow cytometry histogram profiles of RAW 264.7 cells that were pre-incubated with (a-b) 0, (c-d) 80, (e-f) 160 or (g-h) 320 μg/mL **HP-3HF-ArPC** micelles for 12 h. (a,c,e,g for ICT fluorescence channel and b,d,f,h for corresponding IPT fluorescence channel). The percentages shown on histogram profiles represent corresponding gate population of ICT-positive and IPT-positive cells. Overlaid (i) ICT and (j) IPT fluorescence histograms demonstrate that the amount of **HP-3HF-ArPC** micelles uptaken by RAW 264.7 cells increases with the concentration of micelles incubated.

4. Reference

1 A. P. Goodwin, S. S. Lam and J. M. J. Fréchet, *J. Am. Chem. Soc.*, 2007, **129**, 6994.

2 D. P. Sanders, K. Fukushima, D. J. Coady, A. Nelson, M. Fujiwara, M. Yasumoto and J. L. Hedrick, *J. Am. Chem. Soc.*, 2010, **132**, 14724.

3 C.-Y. Chen and C.-T. Chen, *Chem. Commun.*, 2011, **47**, 994.

4 C. B. Tripathi and S. Mukherjee, *J. Org. Chem.*, 2012, **77**, 1592.

5 M. S. Mortensen, J. M. Osbourn and G. A. O'Doherty, *Org. Lett.*, 2007, **9**, 3105.

6 C. Y. Chen and C. T. Chen, *Chem. Eur. J.*, 2013, **19**, 16050.

7 R. C. Pratt, F. Nederberg, R. M. Waymouth and J. L. Hedrick, *Chem. Commun.*, 2008, 114.

8 E. A. Ilardi, C. E. Stivala and A. Zakarian, *Org. Lett.*, 2008, **10**, 1727.

9 J. M. Jego, B. Carboni and M. Vaultier, *J. Organomet. Chem.*, 1992, **435**, 1.

10 A. C. Engler, J. M. W. Chan, D. J. Coady, J. M. O'Brien, H. Sardon, A. Nelson, D. P. Sanders, Y. Y. Yang and J. L. Hedrick, *Macromolecules*, 2013, **46**, 1283.

11 A. M. Brouwer, *Pure Appl. Chem.*, 2011, **83**, 2213.

5. ^{1}H and ^{13}C spectra of TMC monomers, fluorescent ROP initiator and amphiphilic triblock polycarbonates

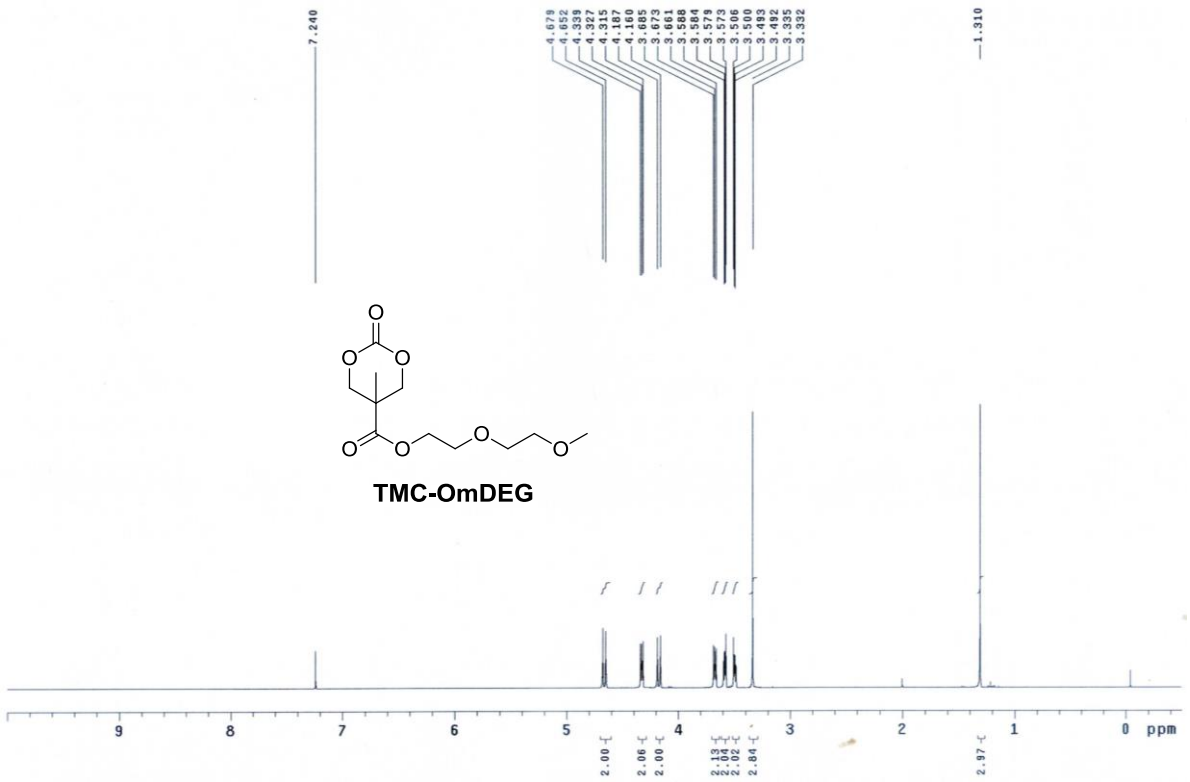

Fig. S12 ^{1}H NMR spectrum (400 MHz) of compound **TMC-OmDEG** in $CDCl_3$

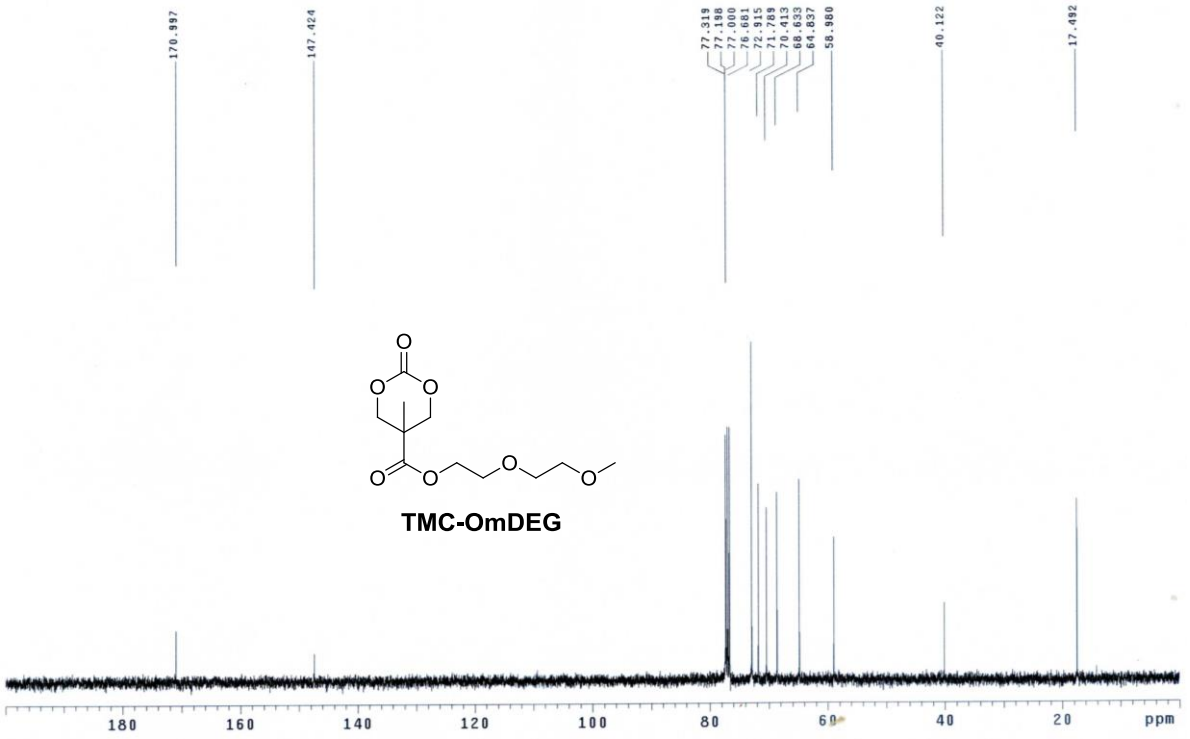

Fig. S13 ^{13}C NMR spectrum (100 MHz) of compound **TMC-OmDEG** in $CDCl_3$

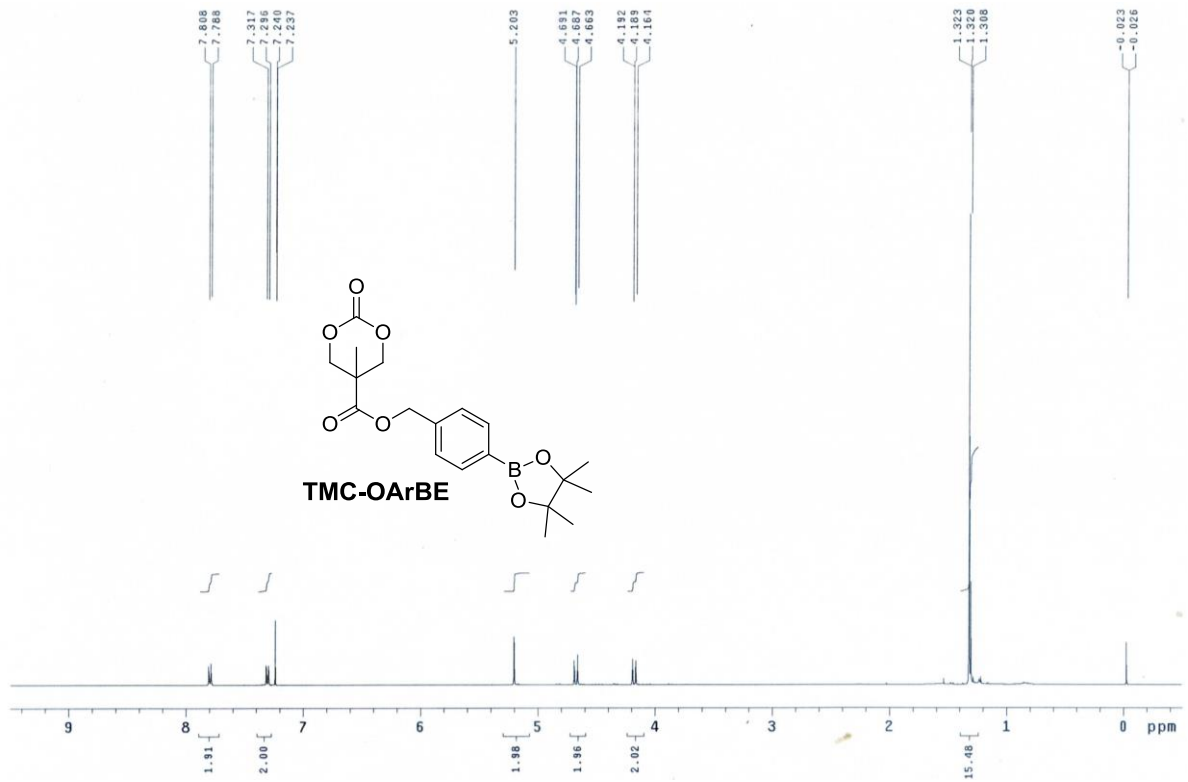

Fig. S14 ^{1}H NMR spectrum (400 MHz) of compound **TMC-OArBE** in $CDCl_3$

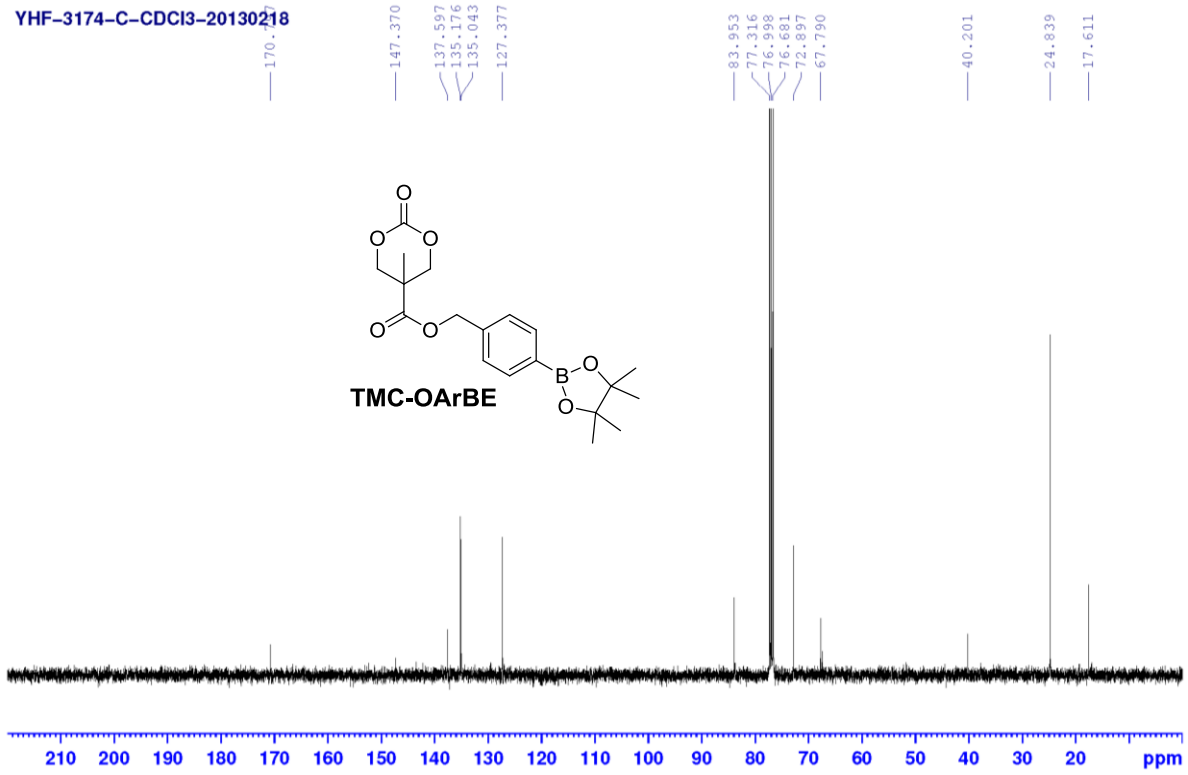

Fig. S15 ^{13}C NMR spectrum (100 MHz) of compound **TMC-OArBE** in $CDCl_3$

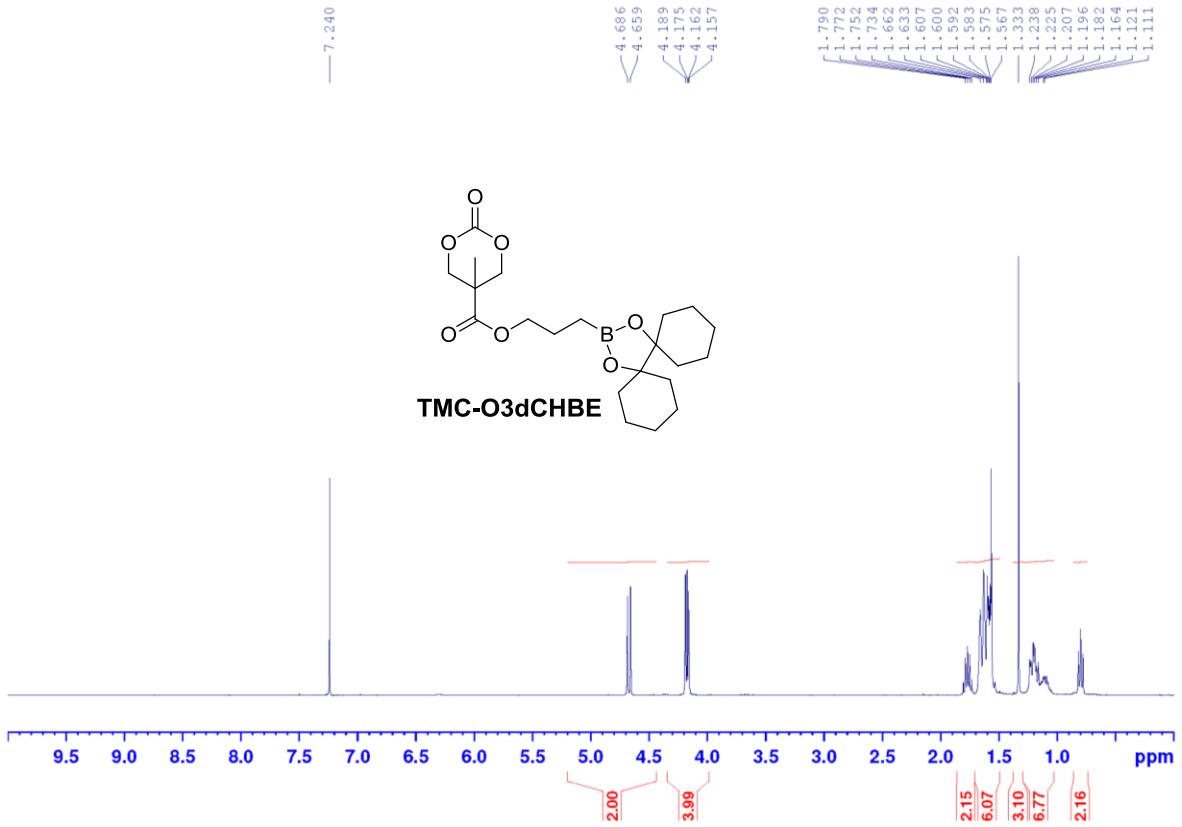

Fig. S16 ^{1}H NMR spectrum (400 MHz) of compound **TMC-O3dCHBE** in $CDCl_3$

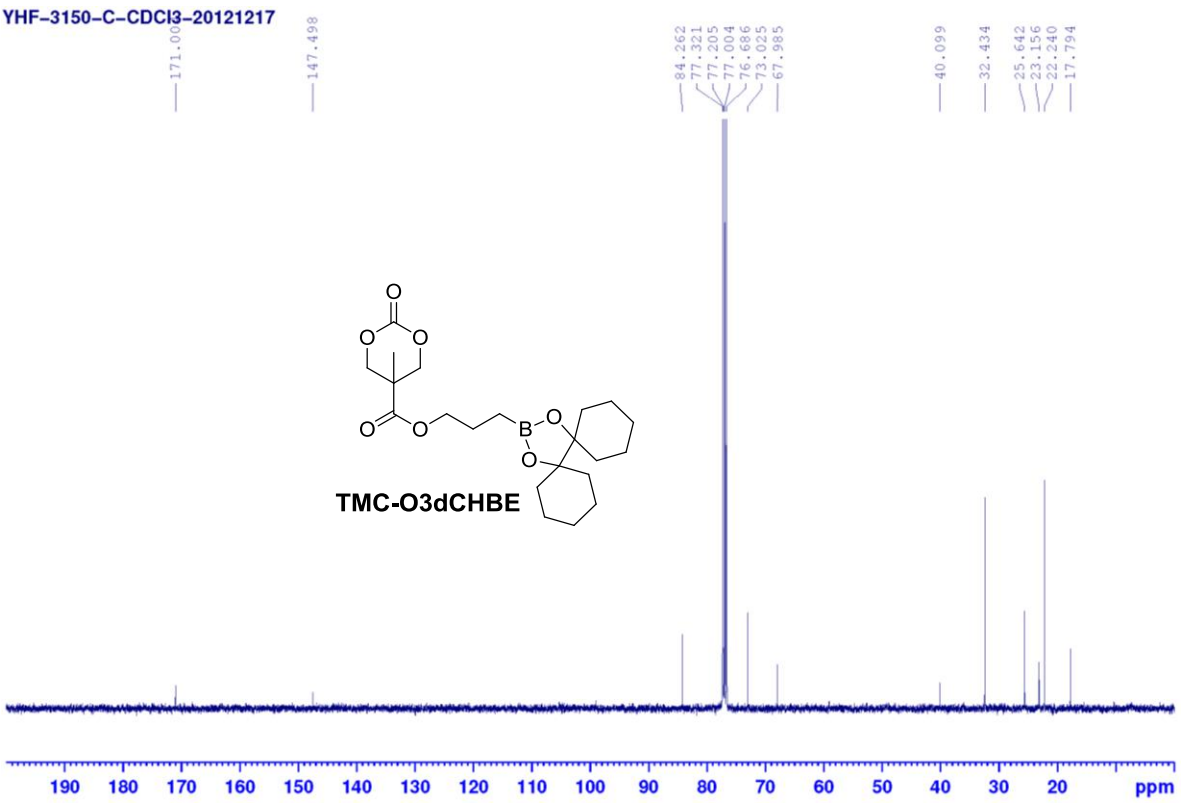

Fig. S17 ^{13}C NMR spectrum (100 MHz) of compound **TMC-O3dCHBE** in $CDCl_3$

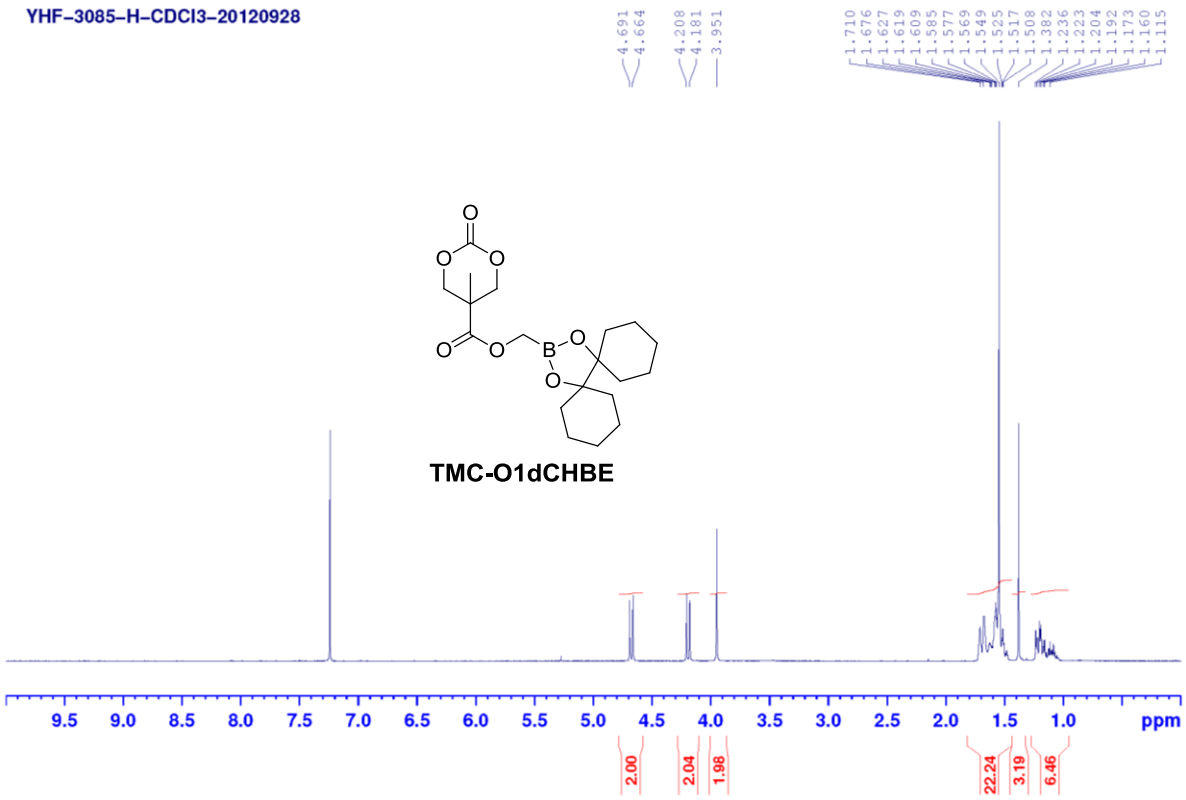

Fig. S18 ^{1}H NMR spectrum (400 MHz) of compound **TMC-O1dCHBE** in $CDCl_3$

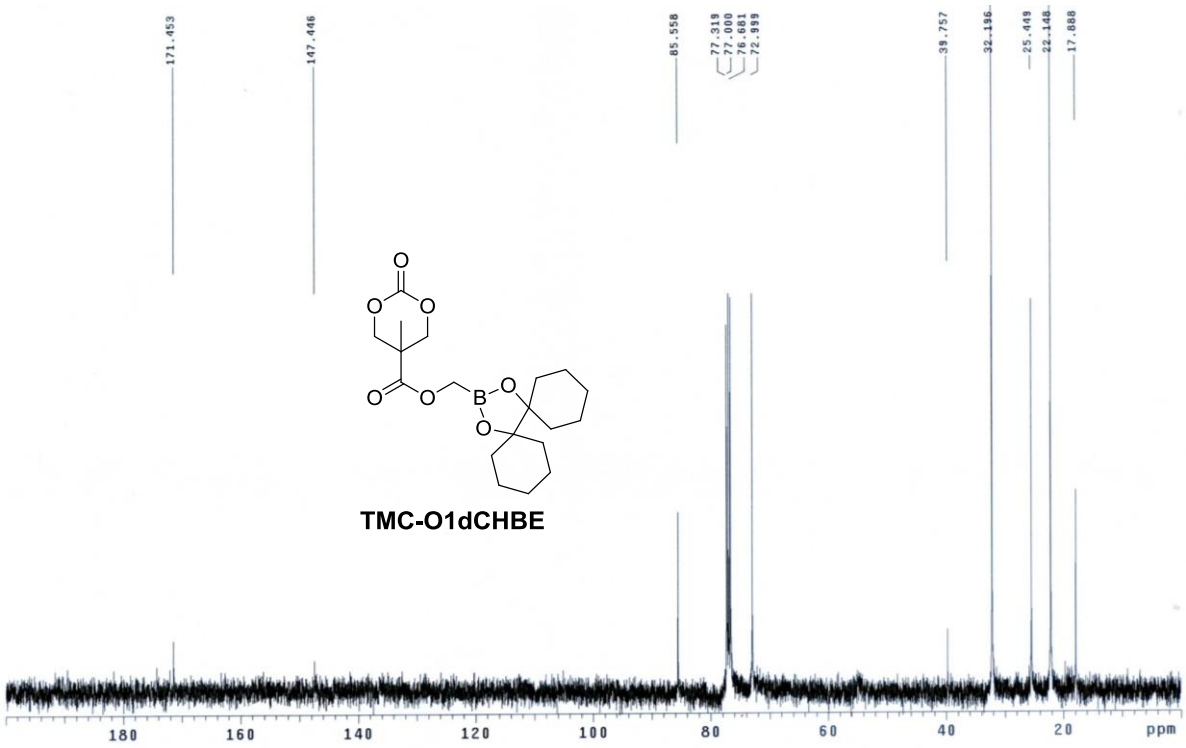

Fig. S19 ^{13}C NMR spectrum (100 MHz) of compound **TMC-O1dCHBE** in $CDCl_3$

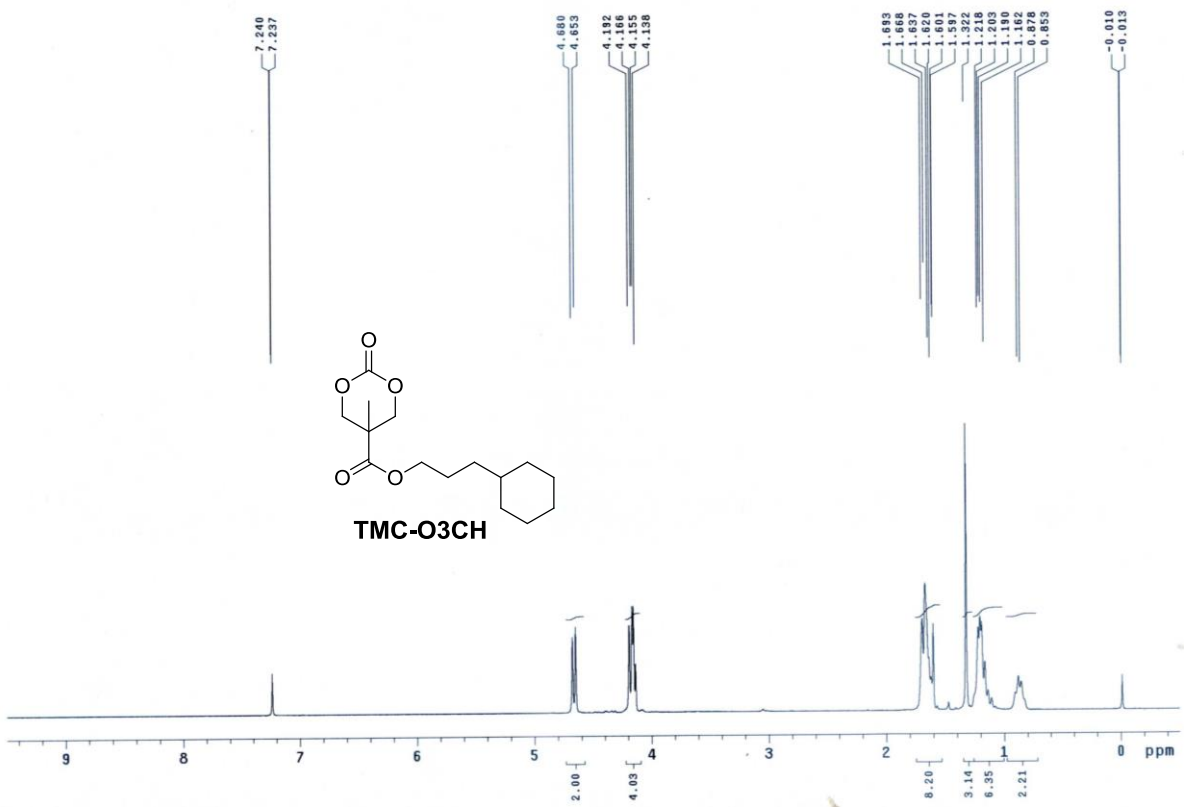

Fig. S20 ^{1}H NMR spectrum (400 MHz) of compound **TMC-O3CH** in $CDCl_3$

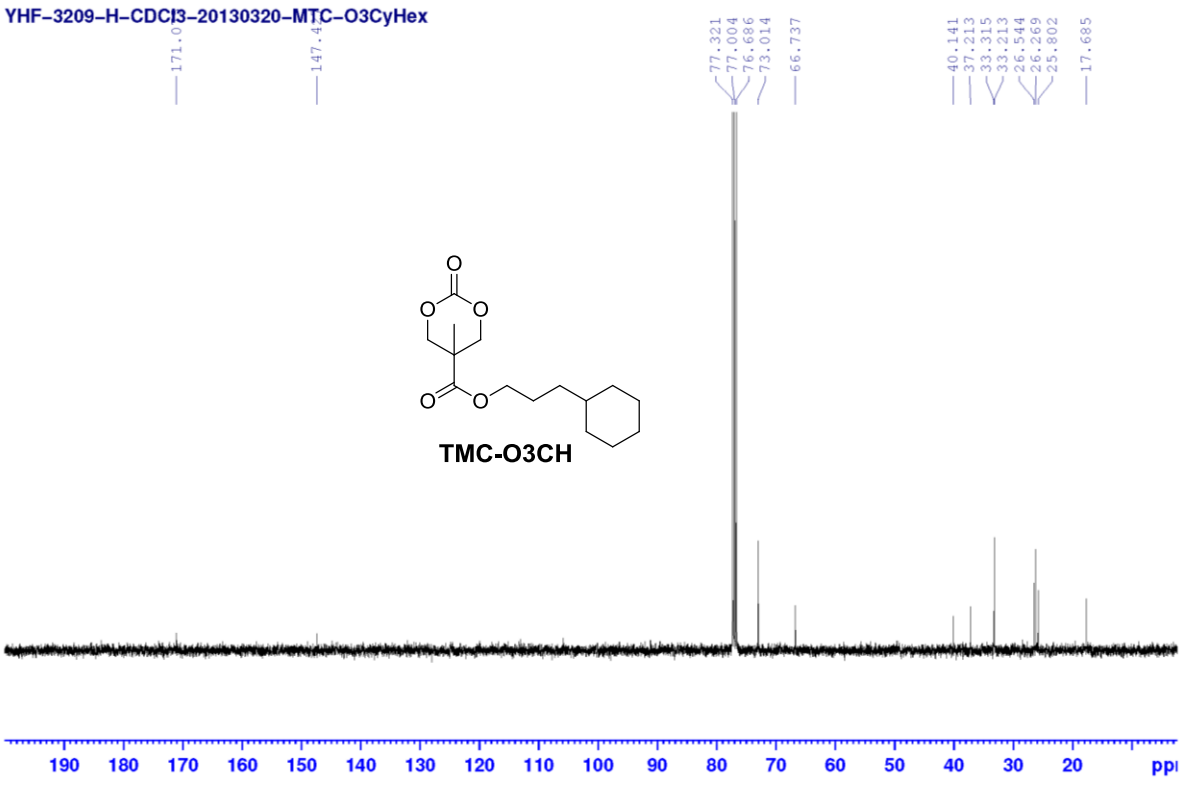

Fig. S21 ^{13}C NMR spectrum (100 MHz) of compound **TMC-O3CH** in $CDCl_3$

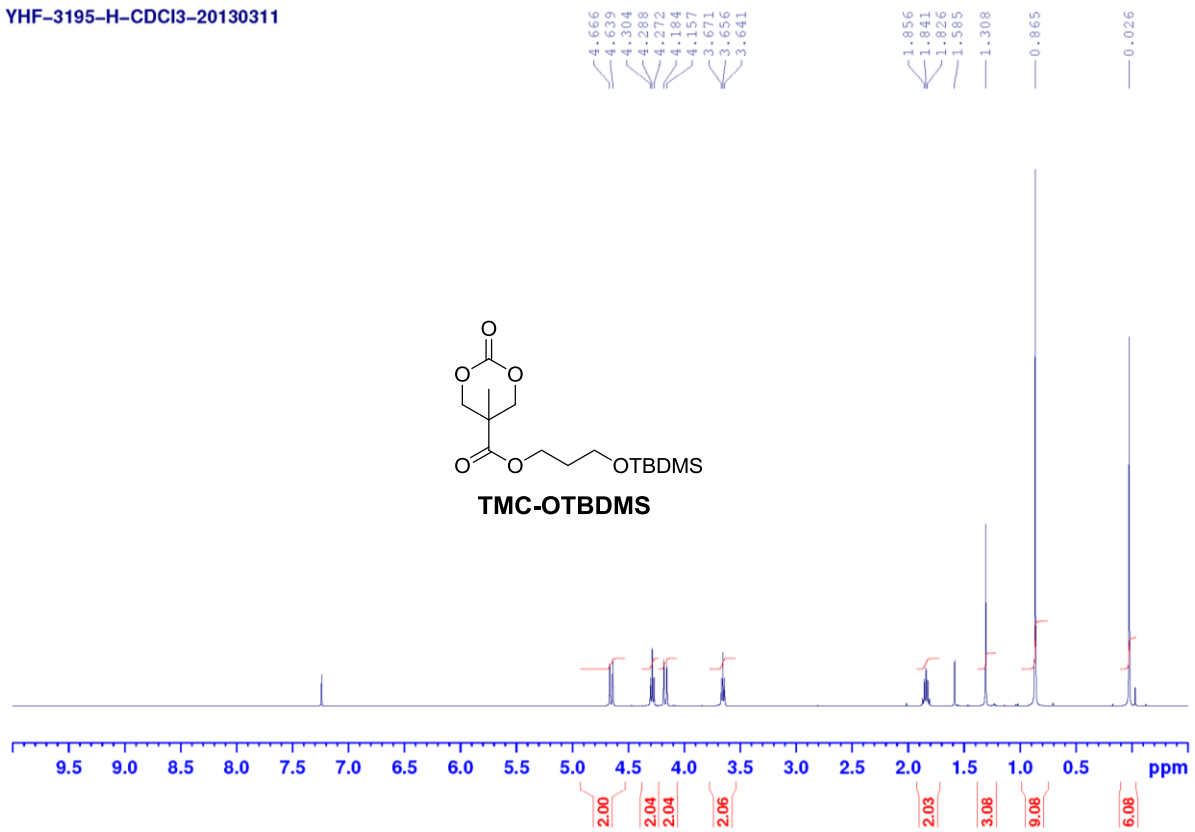

Fig. S22 ^{1}H NMR spectrum (400 MHz) of compound **TMC-OTBDMS** in $CDCl_3$

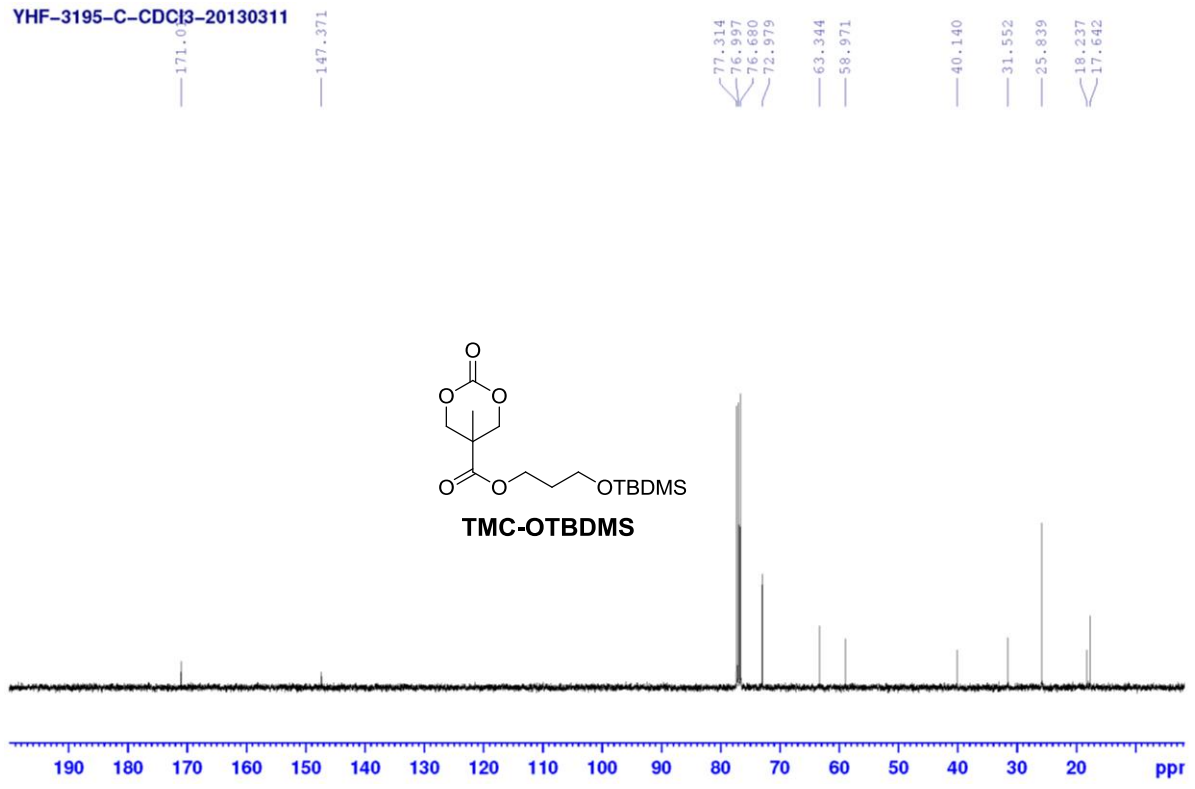

Fig. S23 ^{13}C NMR spectrum (100 MHz) of compound **TMC-OTBDMS** in $CDCl_3$

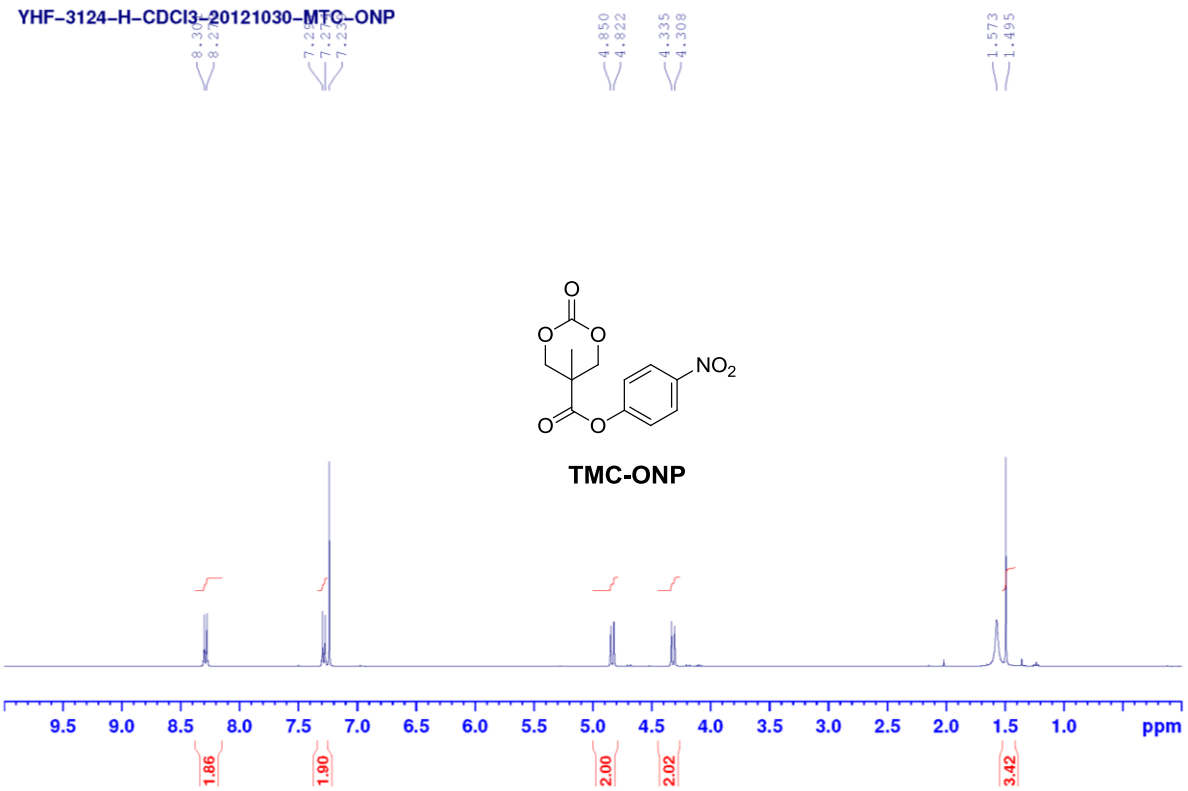

Fig. S24 ^{1}H NMR spectrum (400 MHz) of compound **TMC-ONP** in $CDCl_3$

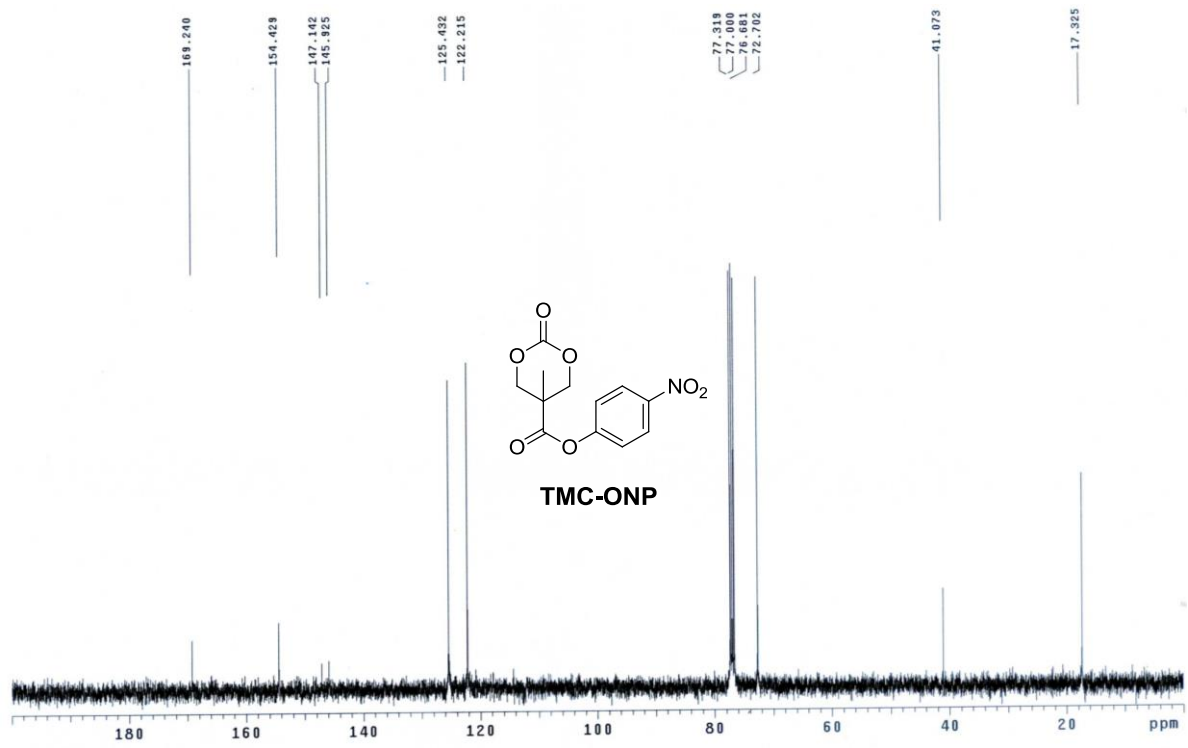

Fig. S25 ^{13}C NMR spectrum (100 MHz) of compound **TMC-ONP** in $CDCl_3$

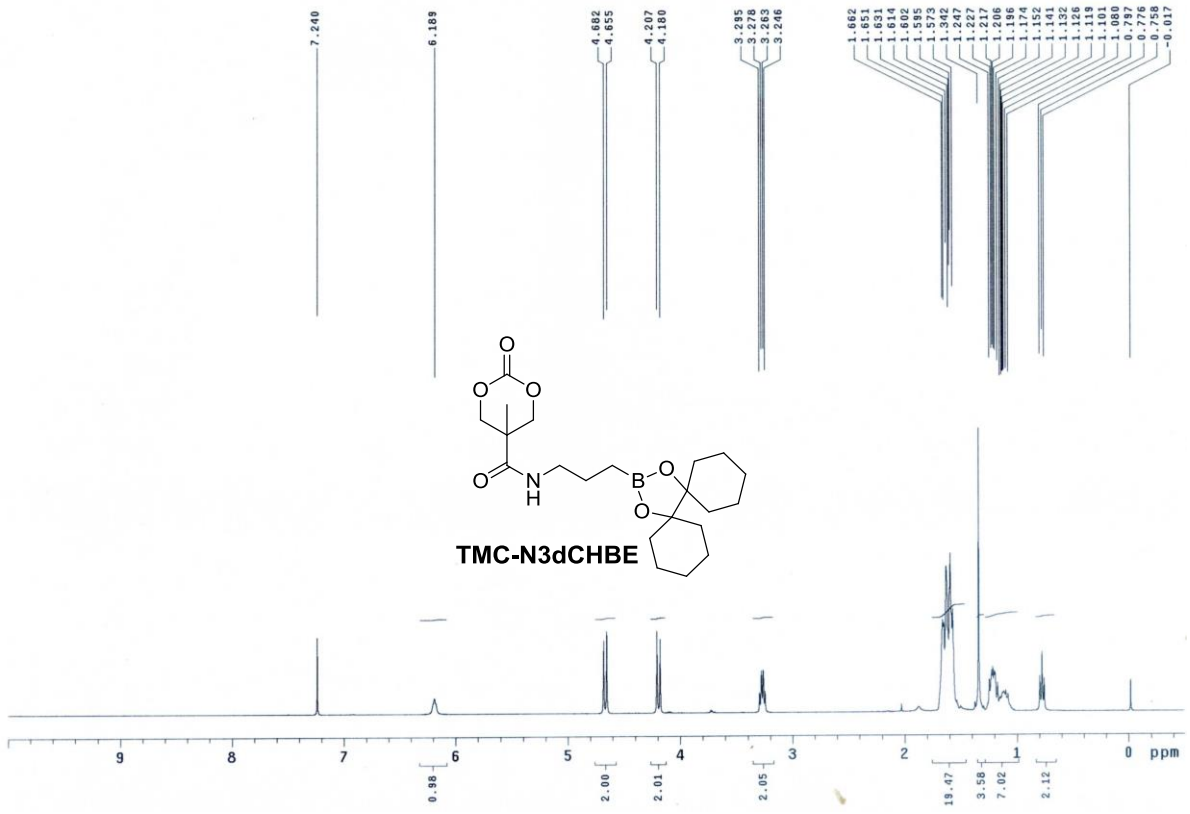

Fig. S26 ^{1}H NMR spectrum (400 MHz) of compound **TMC-N3dCHBE** in $CDCl_3$

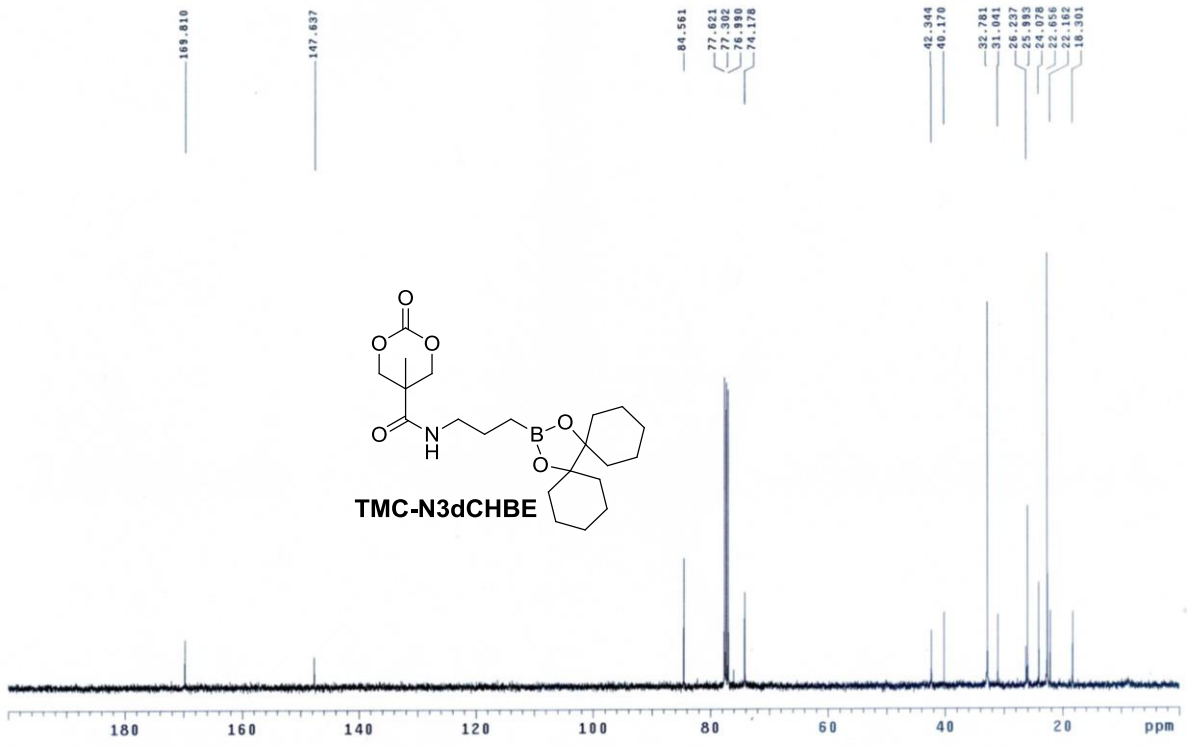

Fig. S27 ^{13}C NMR spectrum (100 MHz) of compound **TMC-N3dCHBE** in $CDCl_3$

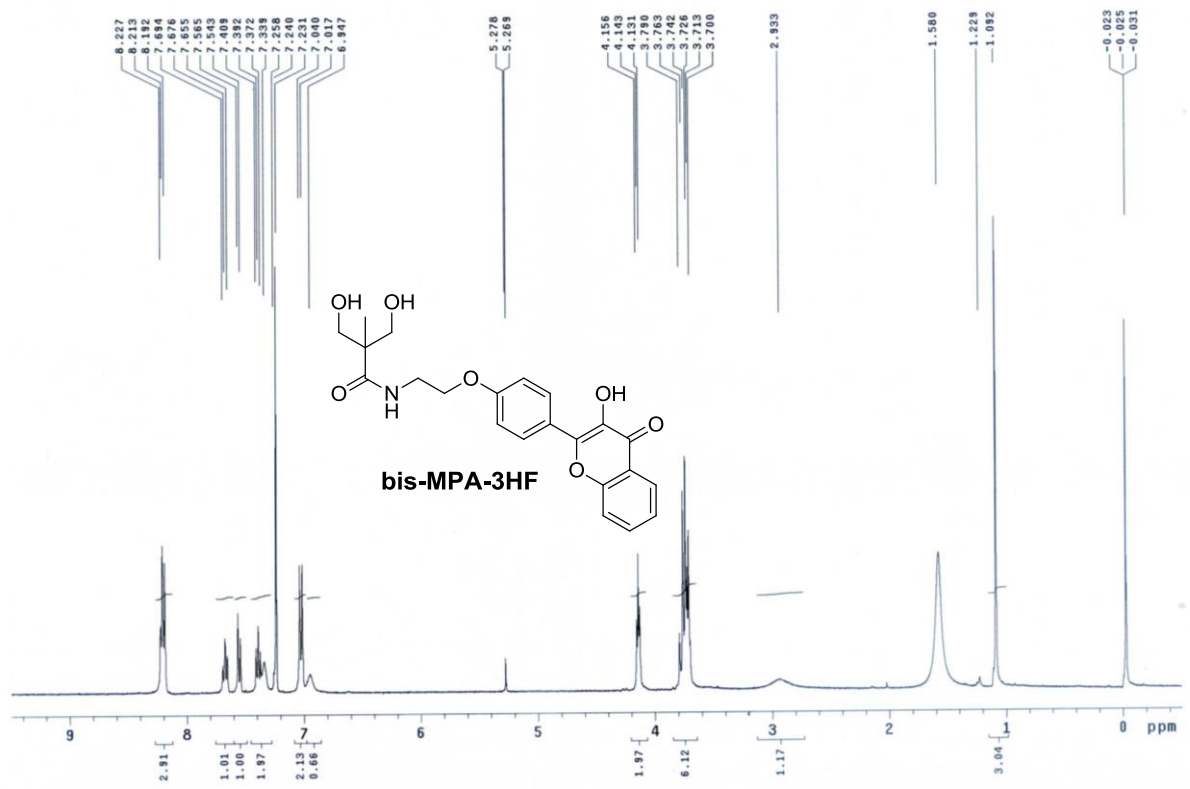

Fig. S28 ^{1}H NMR spectrum (400 MHz) of compound **bis-MPA-3HF** in $CDCl_3$

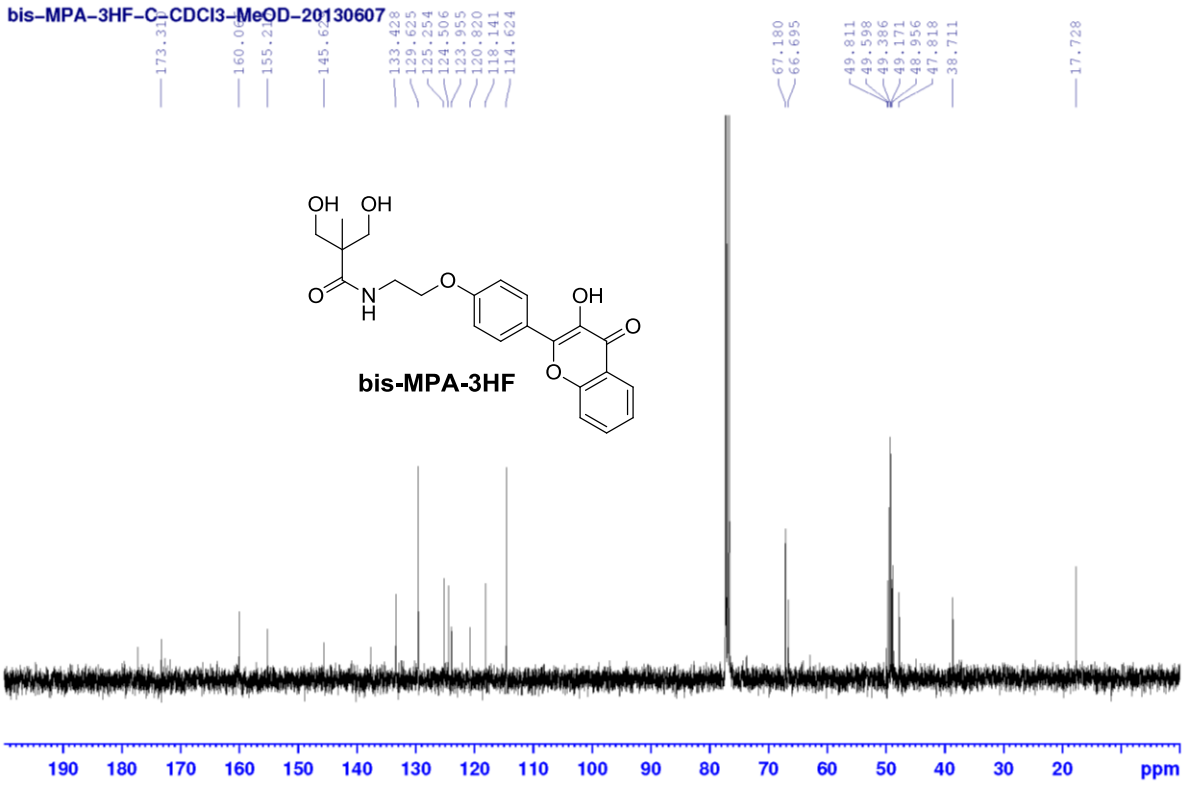

Fig. S29 ^{13}C NMR spectrum (100 MHz) of compound **bis-MPA-3HF** in $CDCl_3$

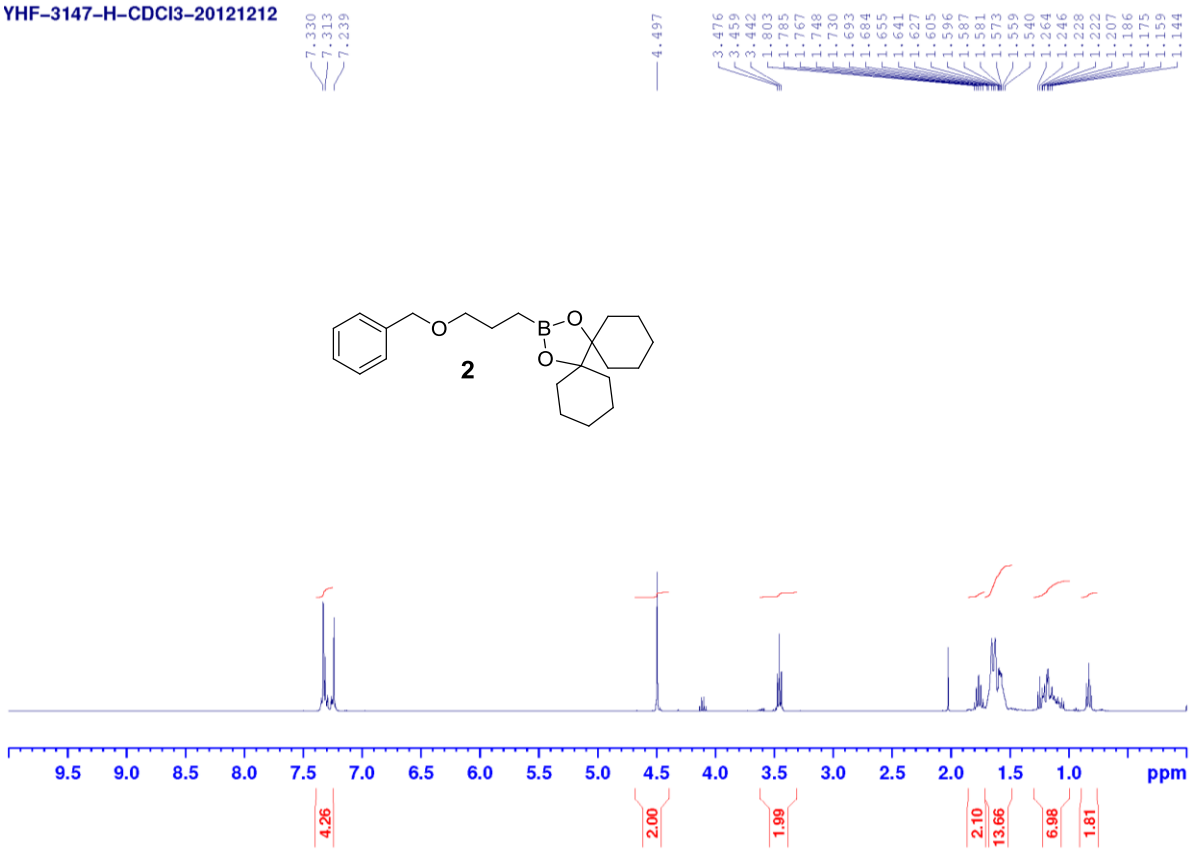

Fig. S30 ^{1}H NMR spectrum (400 MHz) of compound **2**in $CDCl_3$

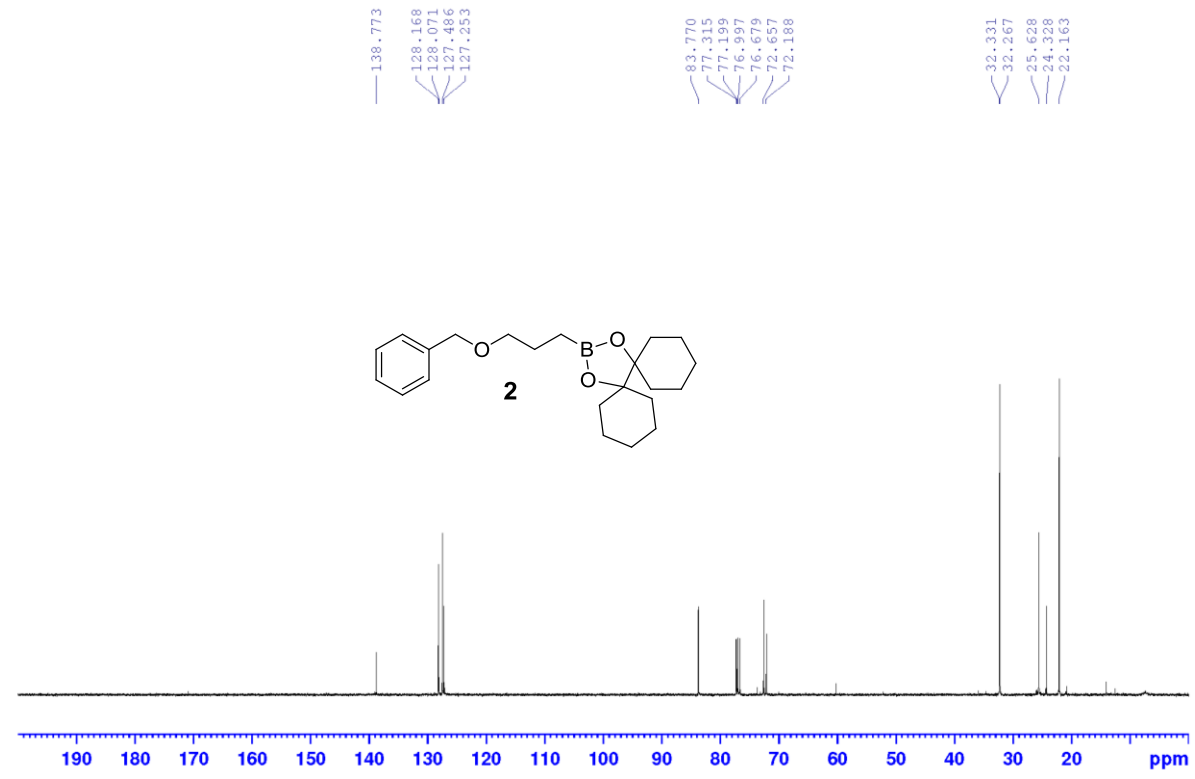

Fig. S31 ^{13}C NMR spectrum (100 MHz) of compound **2** in $CDCl_3$

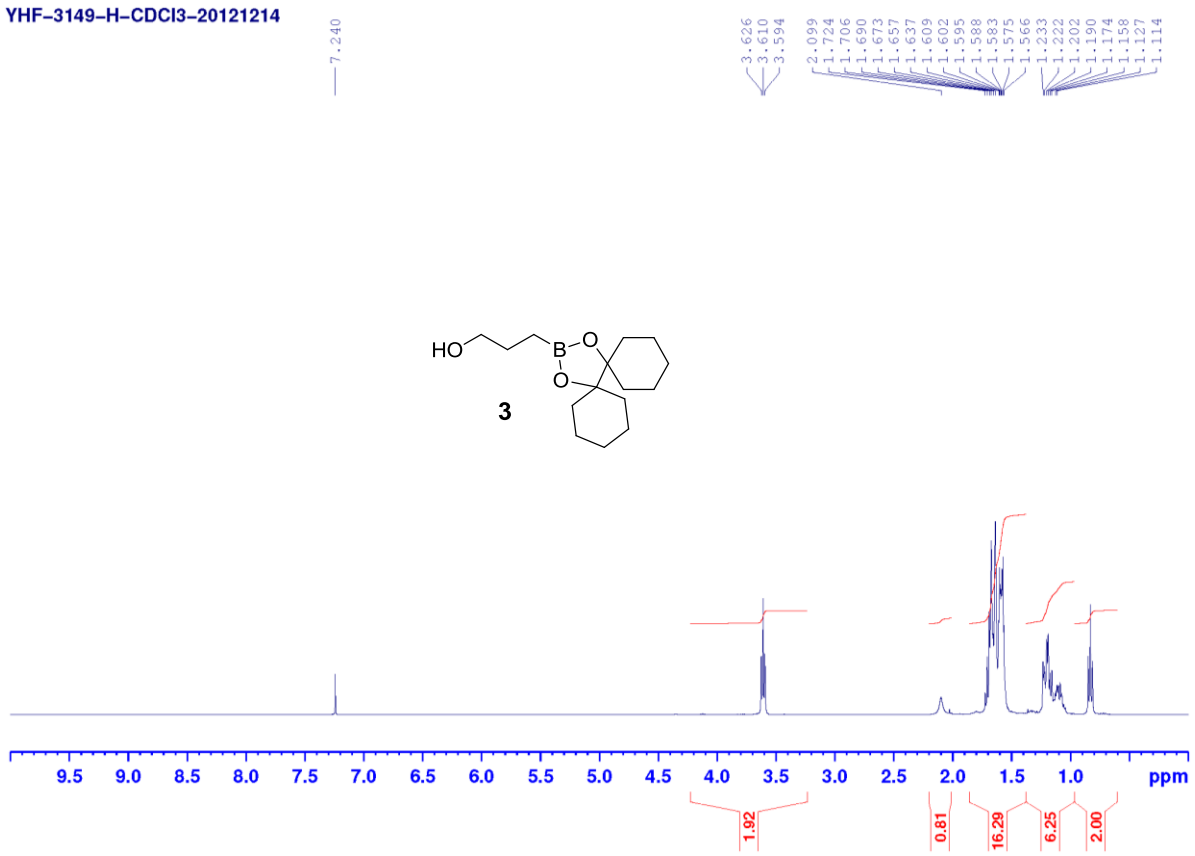

Fig. S32 ^{1}H NMR spectrum (400 MHz) of compound **3** in $CDCl_3$

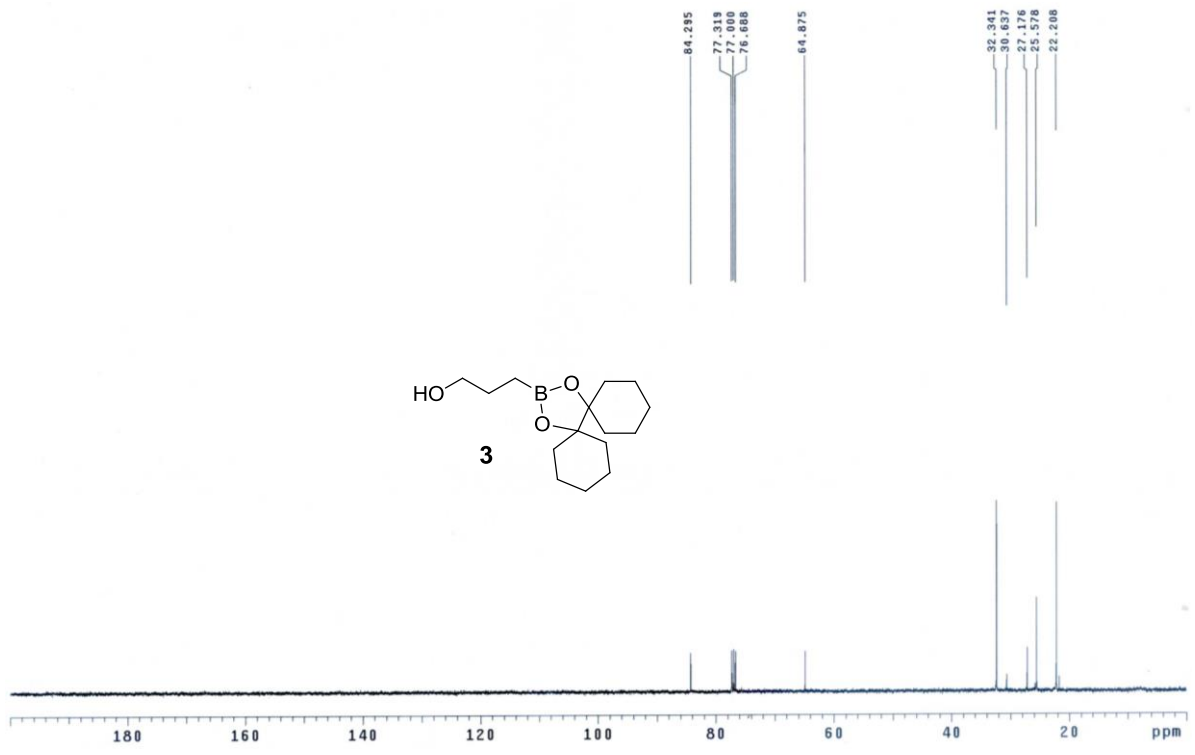

Fig. S33 ^{13}C NMR spectrum (100 MHz) of compound **3** in $CDCl_3$

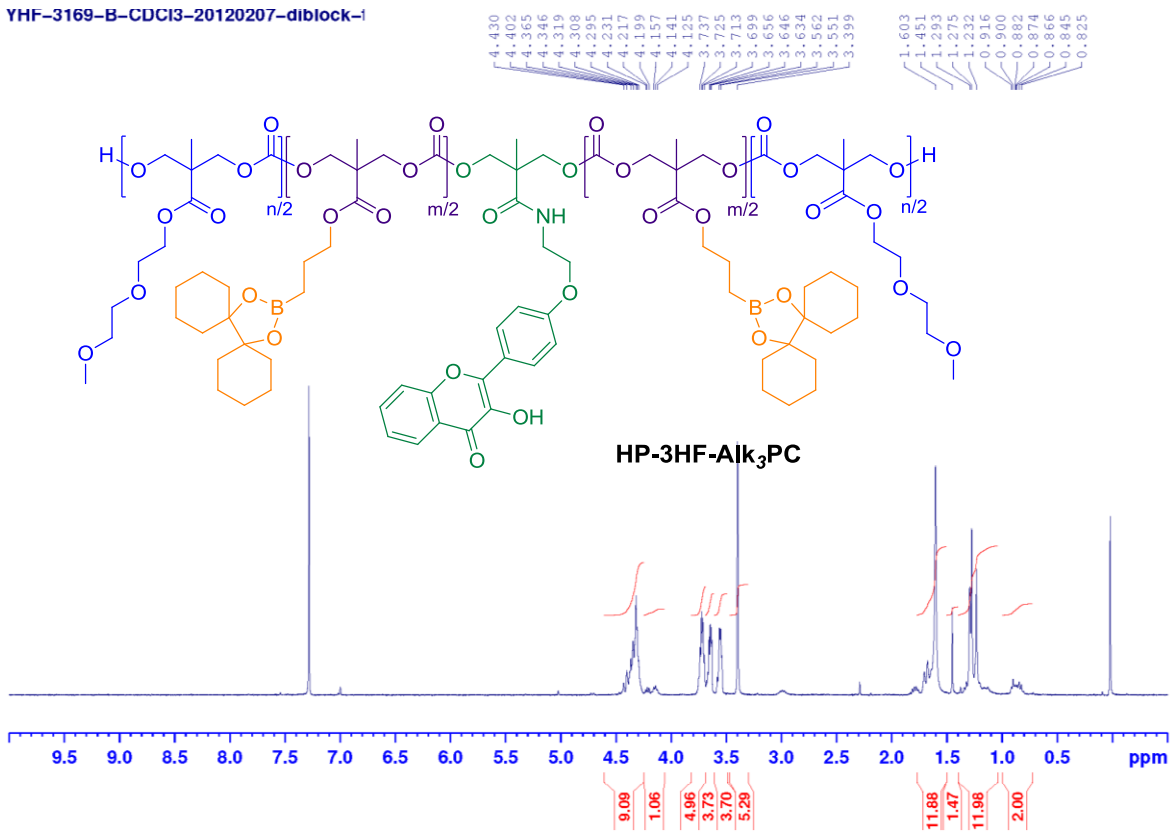

Fig. S34 ^{1}H NMR spectrum (400 MHz) of **HP-3HF-Alk$_3$PC** polycarbonate in $CDCl_3$

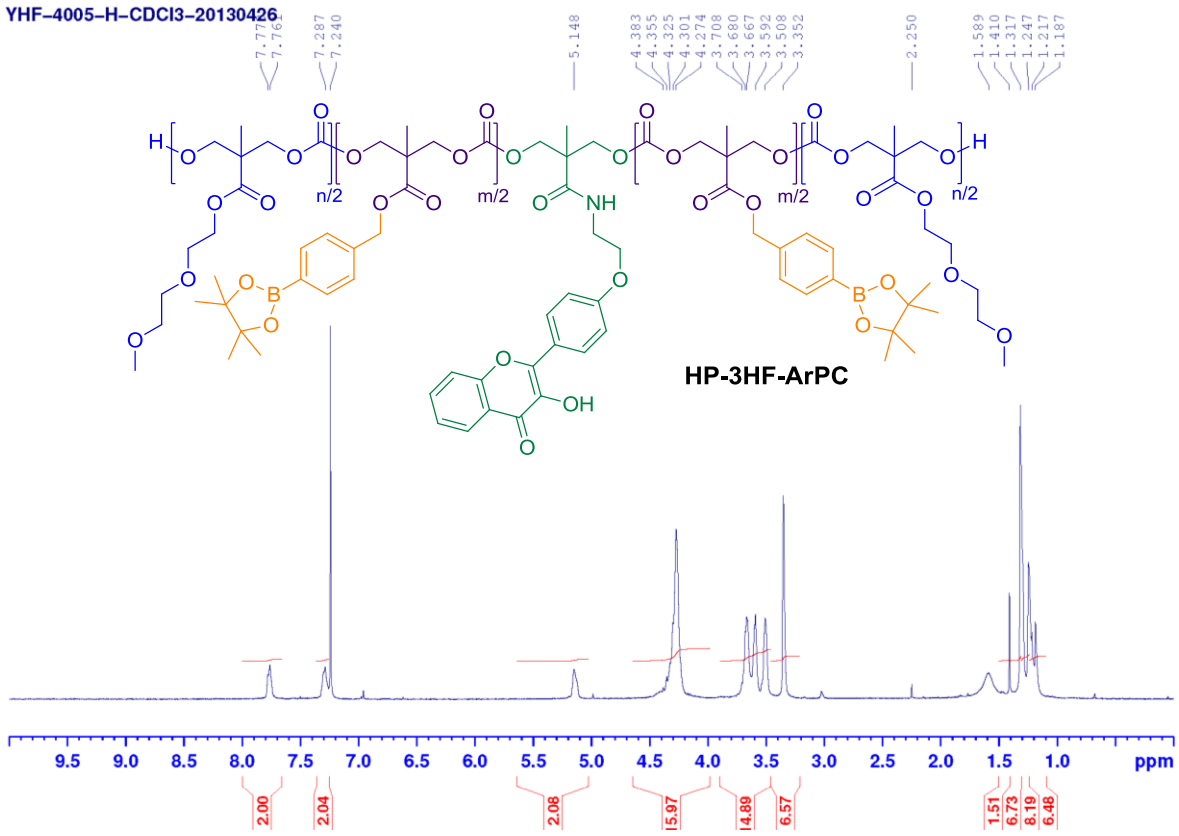

Fig. S35 ^{1}H NMR spectrum (400 MHz) of **HP-3HF-ArPC** polycarbonate in $CDCl_3$

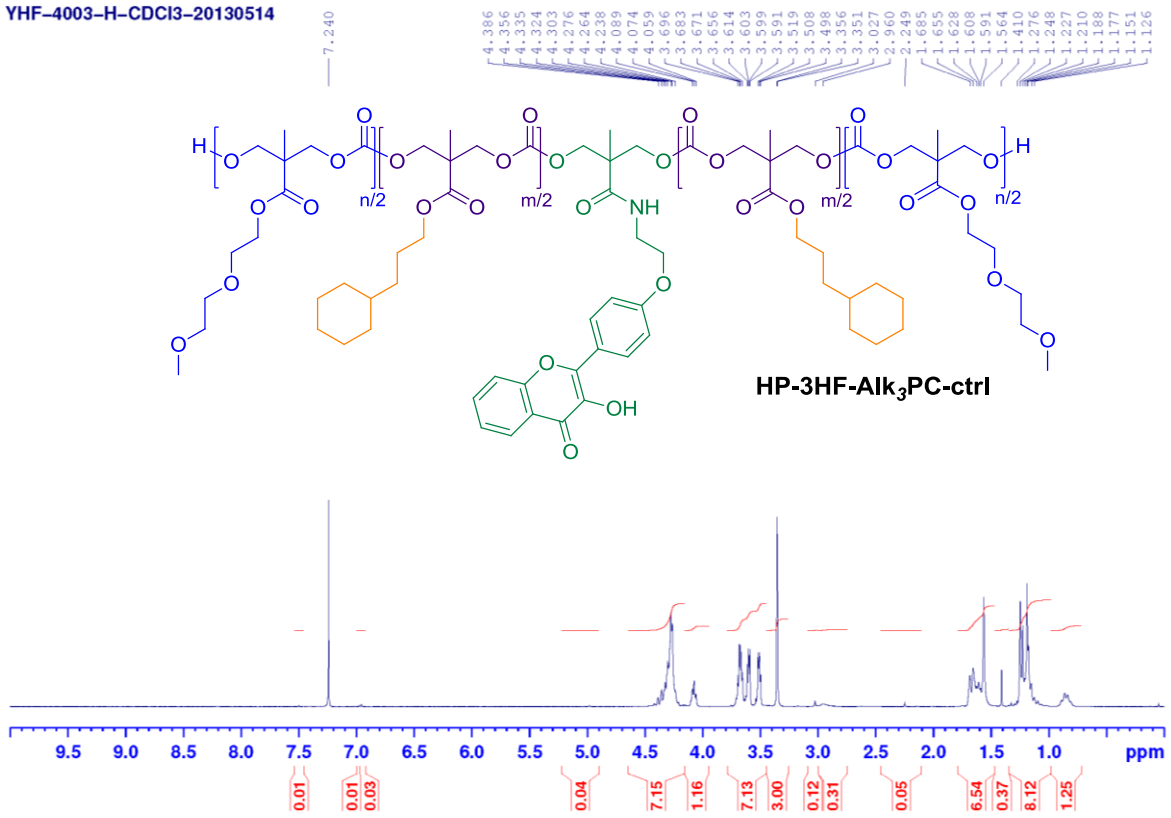

Fig. S36 ^{1}H NMR spectrum (400 MHz) of **HP-3HF-Alk$_3$PC-ctrl** polycarbonate in $CDCl_3$

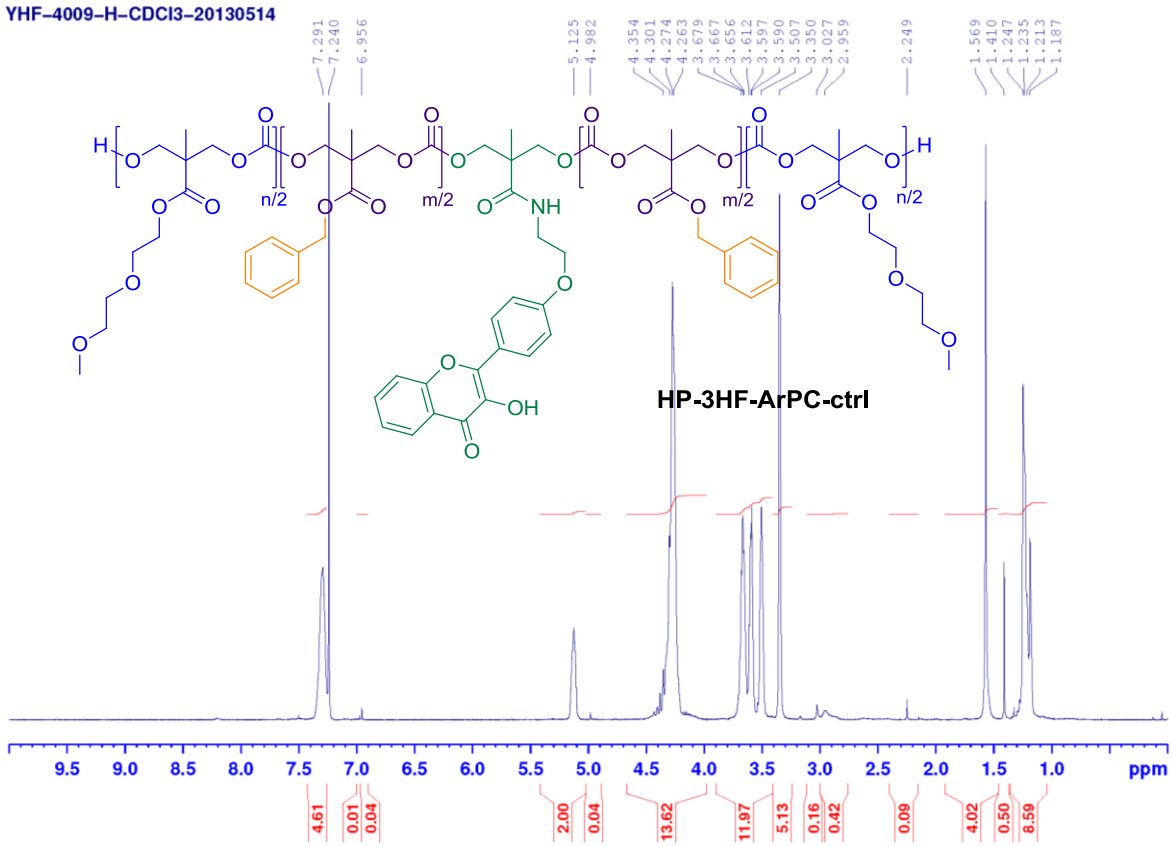

Fig. S37 ^{1}H NMR spectrum (400 MHz) of **HP-3HF-ArPC-ctrl** polycarbonate in $CDCl_3$

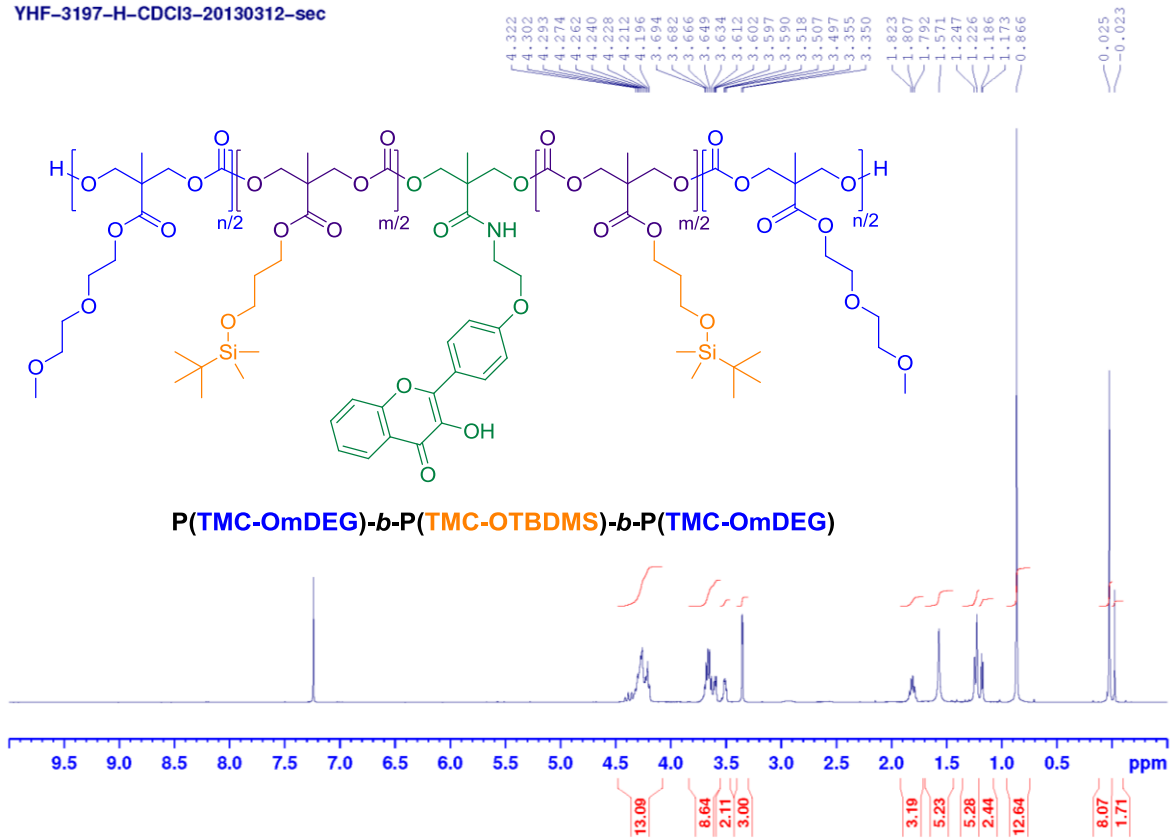

Fig. S38 ^{1}H NMR spectrum (400 MHz) of **P(TMC-OmDEG)-*b*-P(TMC-OTBDMS)-*b*-P(TMC-OmDEG)** triblock polycarbonate in $CDCl_3$